Chemosphere 352 (2024) 141303

Contents lists available at ScienceDirect

Chemosphere

journal homepage: www.elsevier.com/locate/chemosphere

Transport and deposition of radionuclides from northern Africa to the southern Iberian Peninsula and the Canary Islands during the intense dust intrusions of March 2022

Esperanza Liger [a,b,*], Francisco Hernández [b,c], Francisco Javier Expósito [c], Juan Pedro Díaz [c], Pedro A. Salazar-Carballo [d,e], Elisa Gordo [b,f], Cristina González [g], María López-Pérez [d]

[a] Departamento de Física Aplicada II, Universidad de Málaga, Spain
[b] Grupo de Geoquímica y Radiactividad Ambiental, Universidad de Málaga, Spain
[c] Grupo de Observación de la Tierra y la Atmósfera, Universidad de La Laguna, Spain
[d] Laboratorio de Física Médica y Radioactividad Ambiental, SEGAI, Universidad de La Laguna, Spain
[e] Departamento de Medicina Física y Farmacología, Universidad de La Laguna, Spain
[f] Servicios Centrales de Apoyo a la Investigación, Universidad de Málaga, Spain
[g] Instituto Universitario de Enfermedades Tropicales y Salud Pública de Canarias. Universidad de La Laguna, Spain

HIGHLIGHTS

- Two atypical and intense dust Saharan events affected Spain during March 2022.
- These Saharan dust events caused increments of radionuclides in atmospheric aerosols.
- Record concentrations of ^{137}Cs were recorded during these events in Málaga.
- PM10, ^{137}Cs, ^{40}K and gross alpha concentrations correlated during these dust events.
- Rainfall enhanced aerosols deposition to approximately 26–56 days of dry deposition.

GRAPHICAL ABSTRACT

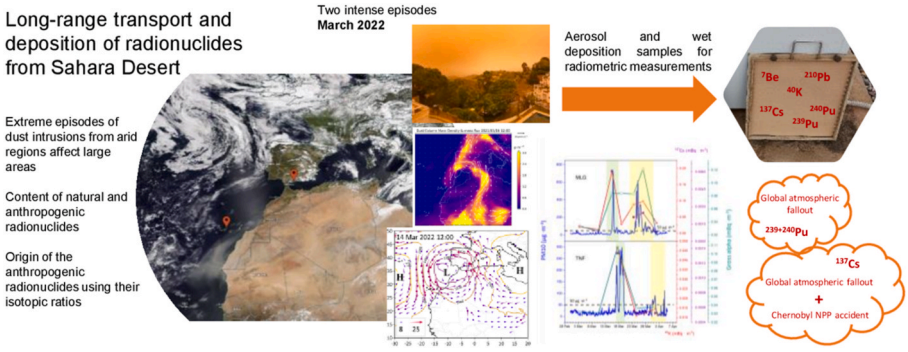

ARTICLE INFO

Handling editor: Milena Horvat

Keywords:
Saharan dust
Long-range transport
Caesium
Plutonium
Aerosol
Atmospheric deposition

ABSTRACT

The present study focuses on the two consecutive and markedly intense Saharan dust intrusion episodes that greatly affected southern Spain (Málaga) and, to a lesser extent, the Canary Islands (Tenerife), in March 2022. These two episodes were the result of atypical meteorological conditions in the region and resulted in record levels of aerosols in the air at the Málaga location. The activity levels of various natural and artificial radionuclides (^{7}Be, ^{210}Pb, ^{40}K, ^{137}Cs, ^{239}Pu, ^{240}Pu, $^{239+240}$Pu) and radioactive indicators (gross alpha and gross beta) were impacted by these events and the results are described herein. These episodes caused, for example, the activities of ^{137}Cs in aerosol samples at the Málaga monitoring station to reach the highest concentrations ever recorded since high-volume aerosol monitoring started at this site in 2009. A link between the activity levels of

* Corresponding author. PDI, Profesora Titular Universidad Departamento de Física Aplicada II Escuela de Ingenierías Industriales C/Arquitecto Francisco Peñalosa, 6 29071 Málaga, Spain.
E-mail address: eliger@uma.es (E. Liger).

https://doi.org/10.1016/j.chemosphere.2024.141303
Received 23 November 2023; Received in revised form 14 January 2024; Accepted 24 January 2024
Available online 25 January 2024

^{137}Cs, ^{40}K and gross alpha in the atmospheric aerosols and daily PM10 concentrations during the episodes is also reported. In addition, isotopic ratios are discussed in the context of the source and destination of the various anthropogenic radionuclides measured. The atmospheric residence time of aerosols during these episodes is also evaluated because it concerns how intrusions to the Canary Islands should be analysed. Finally, for the first time, the concentrations of ^{137}Cs deposition by rainwater during a Saharan dust intrusion are reported and the deposition rate of these radionuclides during these episodes is discussed.

1. Introduction

Dust is considered one of the major sources of tropospheric aerosols in the atmosphere and constitutes an important key parameter in climate studies (Kaufman et al., 2002). Desert dust can be transported over long distances from the source regions (Prospero et al., 2002, 2021). Generally, large-sized particles are deposited near their source, but smaller ones can remain suspended in the air for a few days or even weeks (Rodriguez-Navarro et al., 2018). Large masses of dust transferred during dust outbreaks can lead to higher pollution levels than those arising from average transfer processes. They also produce pollutant fluxes that can be equivalent to the fluxes accumulated over several months or even years. This particularly concerns particle-reactive contaminants such as trace metals and long-lived artificial radionuclides (Eyrolle et al., 2009). The global significance and impact of desert-derived mineral dust aerosol have attracted extensive research focused on analysing dust composition, mineralogy, physical properties, sources, and transport mechanisms (Goudie and Middleton, 2001; Prospero et al., 2002; Scheuvens et al., 2013). Data from these studies have contributed to a better understanding and modelling of dust cycles, and their impact on global atmospheric dynamics, climate, and biogeochemical cycles.

The Sahara Desert is the most important dust source in the world. Approximately 12 % of the Saharan dust moves northwards to Europe, 28 % westwards to the Americas and 60 % southwards to the Gulf of Guinea (Engelstaedter et al., 2006). The frequent occurrence of African dust outbreaks has implications for air pollution regulation strategies and accounts for the marked difference in the features of airborne particulates between Southern and Northern Europe (Rodríguez et al., 2001). Saharan dust transport can greatly increase the ambient levels of aerosols (particulate matter) recorded in air quality monitoring networks (Querol et al., 2009b). This is especially relevant in Southern Europe (Rodríguez et al., 2001; Escudero et al., 2005; Gerasopoulos et al., 2006; Escudero et al., 2007; Koçak et al., 2007; Mitsakou et al., 2008) and in some Atlantic islands (Prospero and Nees, 1986; Chiapello et al., 1995; Arimoto et al., 1997; Viana et al., 2002). Saharan dust outbreaks may also transport microorganisms and anthropogenic pollutants to these locations and directly impact human health (Polymenakou et al., 2008; Rodríguez et al., 2011; Tobías et al., 2011; Karanasiou et al., 2012; Gonzalez-Martin et al., 2018; González-Martín et al., 2021).

Long-term studies on Saharan dust outbreaks have proven to be useful for investigating average dust properties in terms of seasonal patterns and recurrent transport scenarios (Papayannis et al., 2008; Valenzuela et al., 2012; Cachorro et al., 2016; Sicard et al., 2016). Some of these studies have characterised the meteorological situations that favour their occurrence (Salvador et al., 2014; Díaz et al., 2017). Others have focused on the long-range transport of dust using satellite observations or modelling tools (Barreto et al., 2022; Liu et al., 2022). Some publications have analysed the composition of dust, as well as its chemical, microphysical, and physical properties (Moreno et al., 2006; Titos et al., 2017; Rodríguez et al., 2020). Other studies have correlated these episodes to the concentration levels of particulate matter PM10 and PM2.5 (Querol et al., 2019; Çapraz and Deniz, 2021) or the measurement of aerosol optical depth (AOD) from remote sensing instruments (Fernández et al., 2019). Previous long-term investigations have revealed a clear seasonal pattern of Saharan dust events affecting Central Europe based on 218 identified episodes (Varga et al., 2013; Varga, 2020).

Although artificial radionuclides such as ^{137}Cs and transuranic nuclides are commonly observed at ultra-trace levels (10−15 ppm) in the present-day environment, they represent a historical concern for human health protection (United Nations Scientific Committee on the Effects of Atomic Radiation (UNSCEAR, 2000). In terms of the radiological impact of Saharan dust outbreaks, a large deposition of ^{137}Cs, ^{90}Sr, uranium, thorium and plutonium isotopes and ^{241}Am was reported in France as a result of a big Saharan dust storm in February 2004 (Masson et al., 2010). Similarly, a large deposition of ^{137}Cs in Monaco was reported in connection with the arrival of sand from North Africa (Pham et al., 2005, 2017, 2020). The concentrations of radioactive material in seasonal dust storms were studied in the Middle East and Northern African regions (Hamadneh et al., 2015; Aba et al., 2018). Our research team has collected radiometric data associated with over 90, low-altitude, dust intrusions to the Canary Islands since 2001 when the monitoring of atmospheric aerosols started at this site (Hernández et al., 2005a; Hernandez et al., 2007; Karlsson et al., 2008; López-Pérez et al., 2020, 2021). However, studies focusing on the radiological influence of dust intrusions are not unique to the Sahara Desert. Similar dust episodes originating in the Mongolian and Chinese deserts have also been studied in Japan (Igarashi et al., 2005), and the relationship between atmospheric deposition of ^{137}Cs and Asian dust intrusions has been documented (Akata et al., 2007; Fujiwara, 2016). Their findings support the hypothesis that the depositions of anthropogenic radionuclides observed in Japan are primarily the result of long-range transport of Asian dust, rather than local resuspension.

The location of the Iberian Peninsula and the Canary Islands, close to the Sahara Desert, makes these regions prone to dust intrusions of Saharan origin (Goudie and Middleton, 2001; Alonso-Pérez et al., 2007; Gelado-Caballero et al., 2012; Michaelides et al., 2018; Cuevas et al., 2021; Prospero et al., 2021). These dust intrusions are locally called “Calimas” (AEMET, 2022). When these Calimas reach southern Europe, PM10 (particulate matter with a diameter of 10 μm or less) concentrations typically range between 10 and 60 μg m^{-3}. The Saharan dust accounts for, in these cases, between 25 and 50 % of the total PM10 in the air (Rodríguez et al., 2004). However, in March 2022, two spectacular dust episodes occurred. There were reports of red skies and dust deposits across Europe. The WMO Barcelona Dust Regional Center reported PM10 concentrations that were historically high at 107 of Spain’s 471 measurement stations. Some of them exceeded concentrations of 1700 μg m^{-3} (Copernicus). These episodes greatly affected the Andalusia region (Southern Spain, Iberian Peninsula) where the daily recorded PM10 values showed unusually high concentrations in most air quality monitoring stations (Junta_Andalucia), leading in some cases to them exceeding more than 50 times the World Health Organization’s (WHO) latest recommended annual limits of 15 μg m^{-3} in 24 h (WHO).

The aim of this work and additional research currently ongoing at our facilities is to try to understand how Saharan aerosol intrusions impact the presence of various radionuclides in the atmosphere and how the increased concentrations in aerosols impact the soil inventories of anthropogenic radionuclides (López-Pérez et al., 2021, 2022). Ultimately, the aim is to be able to use this radiometric data to better understand environmental processes such as aerosol resuspension, transport, and deposition, which may be critical to modelling the distribution and final destination of radioactive elements after nuclear

accidents. In addition, given the current political instabilities in the world, it is critical to be able to identify whether the source of anthropogenic nuclides in the atmosphere is related to events that took place in the past or new accidental releases of radioactivity. Moreover, extreme weather events have increased globally due to climate change, including extreme temperatures (Intergovernmental Panel on Climate Change (IPCC, 2014). As a result, desert regions are growing. This means that the occurrence of natural dust outbreaks is likely to increase in the future with more important consequences. This is why it is of great importance to understand the potential radiological effects of this type of intense episode.

The two episodes that occurred in March 2022 were related to a specific weather pattern associated with a deep low-pressure system located southwest of the Iberian Peninsula, and a persistent high-pressure area above southern Europe. Because of its virulence, the first episode produced a storm that was even given a name: Storm Celia (AEMET). These conditions provided an efficient pathway for northward aerosol advection (AEMET, 2023). Because of these events, sharp increases in the radioactivity levels in atmospheric aerosols, especially ^{137}Cs and ^{40}K, were recorded by the Málaga (MLG) and Tenerife (TNF) monitoring stations. Similar increases in radioactivity levels, associated with dust outbreaks, have been previously reported for Tenerife (Hernández et al., 2005a; Hernandez et al., 2007; Karlsson et al., 2008; López-Pérez et al., 2020). However, this is the first time that radiometric data are reported for dust intrusion episodes crossing two monitoring locations and two different times during the same period providing a picture of how these events evolved in time.

This present study: 1) reports and compares the content of anthropogenic (^{137}Cs, ^{239}Pu, ^{240}Pu, and $^{239+240}$Pu) and natural (^{7}Be, ^{40}K, ^{210}Pb) radionuclides and gross alpha/beta activity concentrations in atmospheric aerosols, collected at ground level, at the Málaga and Tenerife radiological monitoring stations, as well as aerosol concentrations (PM10) collected at these sites during the two dust episodes; 2) reports the time evolution of the events using supporting data from the Copernicus Atmosphere Monitoring Service, HYSPLIT air mass back-trajectory model (Stein et al., 2015), and NOAA-20 VIIRS True Color Corrected Reflectance and The Modern-Era Retrospective analysis for Research and Applications, Version 2 (MERRA-2) images (Gelaro et al., 2017); 3) reports, for the first time, the concentrations of the above mentioned radionuclides in wet deposition samples collected during such dust intrusion episodes and provides deposition rates; 4) discusses the origin of the said anthropogenic radionuclides using their isotopic ratios and 5) discusses the residence time of the aerosols from these storms as this influences how the origin of Saharan intrusions in the Canary Islands has been characterised in previous studies, using solely back-trajectory models.

1.1. Description of the dust episodes of March 2022

The March 2022 dust outbreaks are characterised by their extreme intensity and duration affecting the entire Iberian Peninsula and later the Canary Islands. The intrusions entered the Peninsula from the southeast. The first episode reached Málaga on March 14th and Tenerife on March 17th. The second episode arrived in Málaga on March 22nd and in Tenerife on March 30th. Both episodes lasted approximately one week and also impacted areas of western, central, and northern Europe. In Fig. 1, the data of the fifth-generation atmospheric reanalysis of the global climate data (ERA5), computed by the European Centre for Medium-Range Weather Forecasts (ECMWF) (C3S), show the geopotential height and wind velocity (above 8 m s^{-1}, approx. 29 km h^{-1}) at 850 hPa level, for the beginning of both dust episodes. The synoptic situation shows a similar scenario leading to these extreme episodes in both situations. A meander in the jet stream gave rise to a deep upper-air trough, close to producing a cut-off low, with the minimum of the geopotential height located over the Gulf of Cadiz and an extensive area of high pressure at the surface over southern Europe.

1.1.1. First episode (MLG: March 14–18th, TNF: March 17–20th)

The formation of the deep low (storm Celia) above Spain is visible in Fig. 1 with the bands of clouds on March 14th and 15th. Clouds from March 16th appeared as very bright white over the Iberian Peninsula, moving to central Europe. The storm Celia and high-cloud remnants above Europe are visible in the figure, hiding the complete detection of the dust's eastward outbreak. The synoptic situation produced an intense flow of air masses from the NW of the African continent towards the Iberian Peninsula that continued towards the Canary Islands. The strong and persistent windstorm, lasting for more than 24 h, significantly contributed to the immense dust cloud that invaded the Peninsula from the second half of the 14th, entering from the southeast. This situation mobilised, and wet-deposited, vast amounts of dust blown from distant areas south of the Sahara.

The optical satellite images in Fig. 1 show the dust through occasional gaps in the cloud, covering some parts of the north of Spain, Portugal, and France. However, precisely because of the cloud cover, the visualisation of the dust plumes, which also affected the whole southern half, centre and east of the Peninsula, is difficult. For this reason, the MERRA2-DUCMASS images are also shown in Fig. 1. They present the true extent of these events illustrating that the first of the dust episodes was continent-wide with a strong input from central Sahara and is — at the date of the episode — one of the largest dust intrusions that has ever impacted Europe. In the second half of March 15th, the Celia storm began to lose intensity and started a gradual transition towards the Mediterranean region via the north of the African continent. Celia ceased to be named as such on the synoptic maps on the 16th, so her life cycle barely lasted about 48 h.

The Celia storm remained stationary until the 15th in the area of the Gulf of Cadiz. This caused strong winds and maritime storms over the Canary Islands, as well as heavy rainfall in the provinces of Málaga and Cadiz and affecting various areas of the central part of the Iberian Peninsula.

1.1.2. Second episode (MLG: March 22–31st, TNF: March 30–03rd)

The second episode began on the 22nd of March in a similar way to the previous one, with the development of a deep trough following a curve in the polar jet stream. The minimum of the geopotential height of the system was again over the Gulf of Cadiz. Although the low that developed was not as strong as in the first situation, it did facilitate a massive new intrusion of dust towards SW Europe, aided by a surface anticyclone located in the western Mediterranean. After reaching the Iberian Peninsula on 24 March, the dust mass began a turn across the Atlantic, finally reaching the Canary Islands on 29 March. In the satellite images, once again, the extensive cloud cover associated with the low prevents the invasion of dust over the peninsula from being clearly seen on the 24th. On the 25th, however, the dust is visible in the SW of the peninsula. On the following days, the 28th and 29th, it is noteworthy how much dust is suspended over the Atlantic and how the synoptic situation generates a cyclonic turn of these air masses until they reach the Canary Islands. Once again, the MERRA2 images show the movement of the dust mass in this episode and its marked intensity. Dust washout episodes deposited yellow-brownish dust material on parked cars, roof windows, and other exposed obstacles.

2. Material and methods

2.1. Sampling sites

Sampling locations of the two radiological monitoring stations relevant to this study are shown in Fig. 2. Both radiological monitoring stations belong to the Radioactivity Environmental Monitoring (REM) network managed by the Spanish Nuclear Security Council (CSN).

The MLG station is in the Mediterranean coastal city of Málaga (SE Spain) which is the second most populous city in the Andalusia region and the southernmost large city in Europe. Málaga is a city of commerce

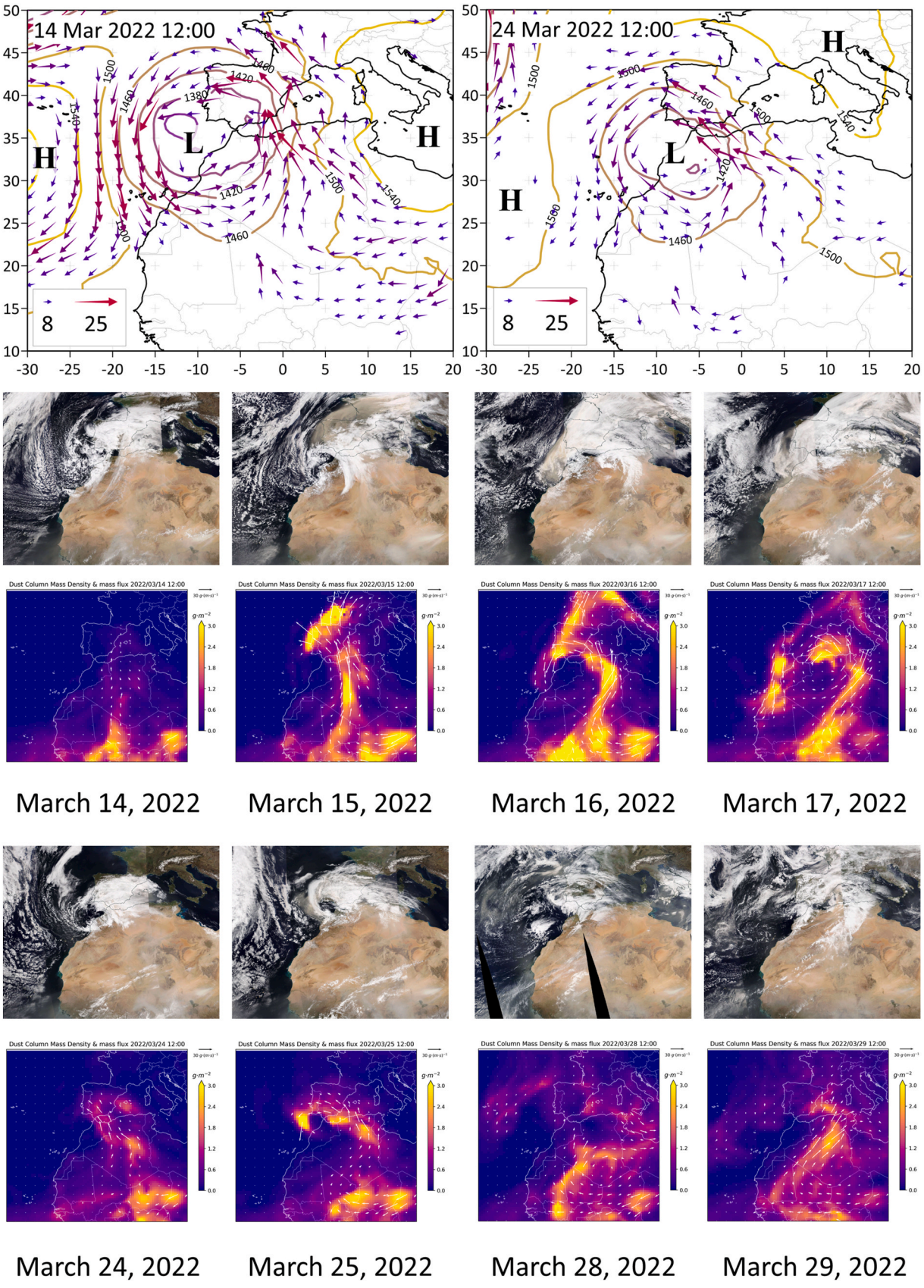

Fig. 1. Geopotential height (mgp) and wind velocity (>8 m s^{-1}) at 850 hPa using ERA5 data on March 14 and 24, 2022 (first row). NOAA-20 VIIRS True Color Corrected Reflectance (2nd and 4th rows) and MERRA2 DUCMASS and flux (3rd and 5th rows) images.

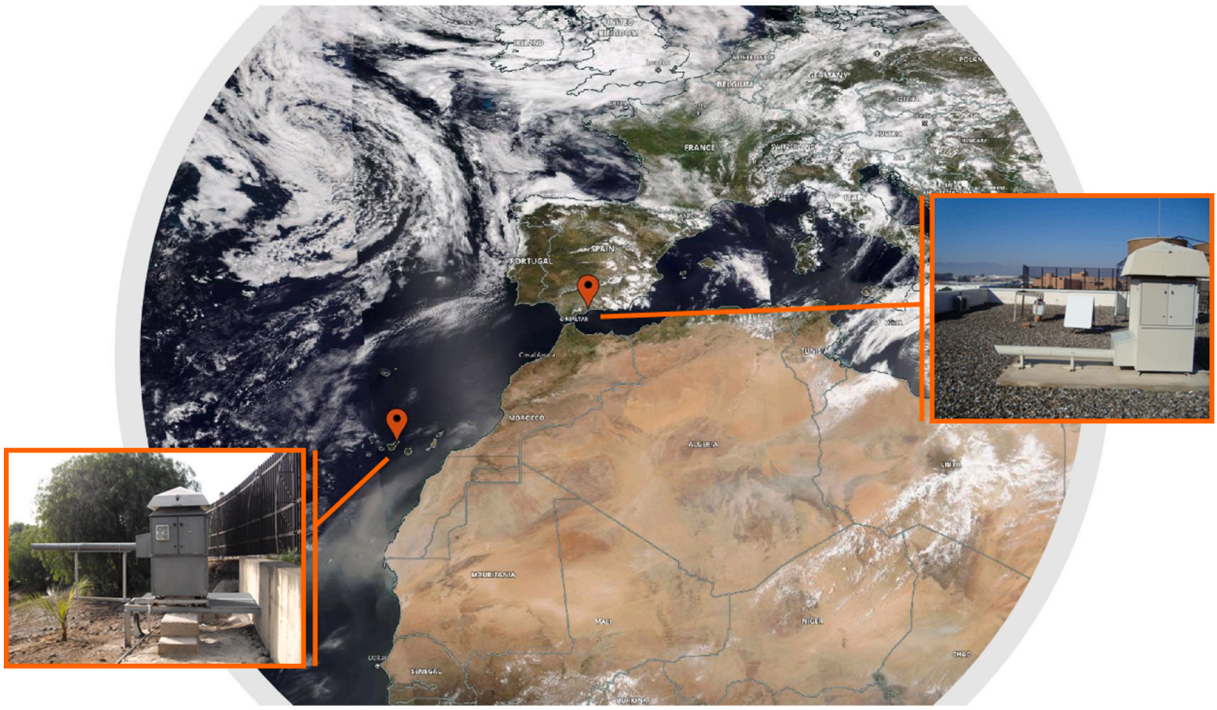

Fig. 2. Map showing the geographical situation of the sampling sites: MLG station at Málaga (4°28′8″W; 36°43′40″N; 10 m.a.s.l.; SE Iberian Peninsula) and TNF station at Tenerife (28° 27′ 29″ N; 16° 17′ 48″ W; 295 m.a.s.l.; Canary Islands). The images depict the high-volume aerosol samplers at each station.

and tourism. Therefore, the local anthropogenic pollutant source is mainly traffic (Amato et al., 2014). The monitoring station is placed in the grounds of the University of Malaga. A detailed description of the MLG station is given elsewhere (Dueñas et al., 1999; Gordo et al., 2015a). There is a clear seasonal trend in this region with a higher frequency of dust outbreaks in May–August, with second modes in March and October (Escudero et al., 2005). Generally speaking, dust storms affecting the western and central Mediterranean are caused by low-pressure systems over the Atlantic or North Africa, high pressure over the Mediterranean, or high pressure at upper levels over NW Africa. In some cases, rain is also present during dry transport events (Querol et al., 2009a; Pey et al., 2013).

The second location, the TNF station, is located in the grounds of the University of La Laguna which is within the Santa Cruz de Tenerife metropolitan area on the island of Tenerife (Canary Islands). The local sources of anthropogenic aerosols at the Tenerife sampling site are limited to emissions from cars and the smoke from two large hospitals, which are within an approximately 1 km radius of the sampling site. A detailed description of the TNF station is given by (Hernández et al., 2005b). At this site, the climate is generally mild, due to the influence of the temperate Atlantic trade winds and the cool waters of the subtropical North Atlantic. Easterly Saharan air episodically reaches the island. These Saharan air masses normally produce an increase in the temperatures and a drop in relative humidity, down to ~15 % (Barbosa et al., 2016). There are two main dust seasons in the Canary Islands, one in winter and the other in summer (Alonso-Pérez et al., 2011). In the winter dust season (November–March), high concentrations of aerosols at ground level (up to 3000 μg m^{-3}) have been registered (López-Pérez et al., 2020; Cuevas et al., 2021). During the summer season (July–August) dust episodes are associated with the circulation of the dusty Saharan Air Layer (SAL) and aerosols generally arrive on the islands at much higher altitudes, >2000 m.a.s.l. (Viana et al., 2002; Barreto et al., 2022).

2.2. Collection of atmospheric aerosol samples

The aerosol sampling and measuring procedures, which were used by both monitoring stations relevant to this study, were the same since both stations belong to the REM network. These are described in detail elsewhere (Hernandez et al., 2007; Gordo et al., 2015a; López-Pérez et al., 2020). Briefly, at each site, two different types of atmospheric aerosol samplers were used to collect total suspended particles: a high-volume sampling station (HVS) type ASS-500 and a low-flow sampling station (LVS), type Radeco, mod. AV-28A.

The HVS are all-weather instruments for the continuous collection of air aerosols (see Fig. 2). The HVS aerosol sampling stations at MLG and TNF are equipped with G3-type polypropylene filters (44 × 44 cm^2). These large filters are folded and pressed to obtain a surface area of approximately 8 × 8 cm^2, with the active area facing inward to prevent loss of material. The mean average airflow for these units for a weekly sampling period is approximately 600 $m^3\,h^{-1}$. However, the air volume in these units can vary as it depends on the aerodynamic burden of the filter with the aerosols collected in it and this ranges from 6E+04 to 1.2E+05 m^3. In the LVS, the airflow is adjusted to collect, under normal conditions, 35 L min^{-1}, although these values fluctuate from week to week depending on the actual atmospheric situation. The low-volume samplers are equipped with a calibrated internal flowmeter and the system automatically records the total volume of sampled air. Cellulose 47 mm diameter filters are used in the low-volume sampler.

During normal radiological situations, the recommended sampling period for these aerosol samplers (HVS and LVS) is one week. However, during the two dust episodes studied herein, HVS filters had to be changed at the MLG station after 2–3 days due to a significant drop in pressure in the air pump. The exact sampling intervals are described in the Supplementary Material (see Table S1).

The particulate matter collected in the various filters during the studied episodes was measured gravimetrically. The filters impacted by the Saharan dust episodes had characteristic yellow-brownish dust deposits (see Fig. S1 in the Supplementary Material for details), which are not present under normal conditions.

2.3. Collection of wet deposition samples

Rainwater samples were only collected during the two strong dust outbreaks that occurred in March 2022 at the MLG station. The first rainwater sample was collected on March 15th coinciding with Storm Celia. The second rainwater sample was collected on the 25th. Both intense episodes produced important wet deposition events that were heavily dust-laden.

Rainwater samples were obtained with a dry/wet deposition collector (ARS 1000 sampler, MTX, Italy) installed next to the HVS and LVS aerosol samplers at the MLG station. Both wet deposition samples (WD) were collected in high-density polyethylene containers with a 540 cm^2 opening equipped with a rain sensor. A movable lid covered the wet deposition container during dry periods and moved to cover the dry container when the rain started. Containers were pre-cleaned by rinsing several times with 500 mL 10 % (v/v) trace-metal grade HCl followed by a rinse with deionized water. Rainwater collectors were deployed on predicted days of rainfall. After the rainfall, the collectors were sealed and returned to the laboratory. The sample collection periods were 1.13 days and 1.23 days, respectively at each of the episodes. These African dust episodes were clearly recognisable because of the brown-reddish drop marks on the white bucket walls. A volume of unfiltered rainwater samples was preserved and used for gamma spectrometry analysis (WD samples).

2.4. Radioactive and radio-chemical analysis

A scintillation detector ZnS(Ag) (MLG station) and low background proportional counters (both stations) were used to determine the gross alpha and gross beta activities, respectively, in the LVS filters. Due to the low radioactivity level of the environmental samples, long counting times (1000 min) were necessary. These measurements were carried out between 3 and 5 days after the sampling to avoid the interference of the short-lived radon daughters. Further details on the technical features of the devices have been described in previous works (Dueñas et al., 1999, 2001; Hernández et al., 2005b).

High-resolution gamma-spectrometry was used to measure gamma-emitting radionuclides (^{7}Be, ^{210}Pb, ^{40}K and ^{137}Cs) in the large filters from the HVS and the unfiltered rainwater samples. Measurements were performed using coaxial-type germanium detectors. Their resolutions were in the range of 1.7–1.8 keV at 1.33 MeV of ^{60}Co. The acquisition times ranged from 2 to 4 days. Reported uncertainties reflect propagated errors arising from 2σ counting error, the detector efficiency calibrations, and the background correction. The background activities of the detectors were monitored and accounted for regularly. Further details of the low-background gamma-ray detection systems used for this study and the calibration of the system for gamma-spectrometry can be found elsewhere (Dueñas et al., 1999, 2004; Hernández et al., 2005b; Gordo et al., 2015a; López-Pérez et al., 2020).

The presence of ^{239}Pu ($t_{1/2}$ = 24,110 yr) and ^{240}Pu ($t_{1/2}$ = 6563 yr) was measured in four of the aerosol samples collected during March 2022. These filters were sent to the Centro Nacional de Aceleradores (CNA) in Seville (Spain) (http://cna.us.es/index.php/en/) to determine the concentration of plutonium isotopes by Accelerator Mass Spectrometry (AMS). In general, AMS determinations involved the chemical isolation of the elements studied from the sample and their adjustment to a specific physical-chemical medium. Details about the ^{239,240}Pu measurement techniques used are described elsewhere (Chamizo et al., 2008, 2015).

2.5. Supporting atmospheric data

Version 4 of the Hybrid, Single-Particle, Lagrangian Integrated Trajectory (HYSPLIT) atmospheric model was used to visualise the pathway of the trajectory of the March 2022 dust episodes (Stein et al., 2015). Four-day back-trajectories were calculated for the air mass arriving at the height of the stations (100 m for Málaga and 300 m for Tenerife), and 1500 m and 2700 m above mean sea level.

The temporal evolution of the desert dust transport and its impact at surface level and in the atmospheric column were also analysed using information obtained from.

- Output of the NMMB/BSC-Dust and BSC-DREAM8b v2.0 models from the Barcelona Dust Forecast Center (WMO)
- Satellite imagery from Meteosat RGB Dust composites
- Output of the Copernicus Atmospheric Monitoring Service (PM2.5 & PM10 concentration maps at surface) (COPERNICUS)
- Aerosol data from the Modern-Era Retrospective analysis for Research and Applications, v.2 (MERRA-2) (NASA)

Ground-level measurements of PM10 load during the dust events were included in the present study and data were retrieved from the nearest stations to the monitoring sites within the two metropolitan areas. The PM10 data ($\mu g \cdot m^{-3}$) refer to hourly concentration measurements. The PM10 monitoring site in Málaga belongs to the Air Quality Monitoring Network of the Regional Government of Andalusia (Carranque; 36.72° N, 4.45° W) (Junta_Andalucia). Details of the PM10 monitoring station considered can be found in (de la Rosa et al., 2010). Publicly available PM10 concentration data were obtained from the Tome Cano monitoring station in Santa Cruz de Tenerife (Tome Cano station; 28°27′43.8″ N; 16°15′42.82″ W, 67 m.a.s.l.), as part of the Air Quality Control and Surveillance Monitoring Network belonging to the Government of the Canary Islands (GOBCAN).

3. Results and discussion

3.1. Aerosol trajectories and PM concentrations

Fig. 3 shows some of the back-trajectories calculated with the HYSPLIT model for key moments during the two March 2022 episodes (mostly when PM10 concentrations started to increase rapidly or peaked at the monitoring sites). The first row of images shows the back-trajectories arriving at the Málaga station in the first episode and seem to indicate that the bulk of the aerosols (PM10) travelled to the MLG site at an altitude between 1000–3000 m.a.s.l. The second episode (second row), although less intense, also followed the previous pattern at the MLG station.

The third and fourth rows of images show the air mass trajectories towards the TNF station for the two episodes. The trajectories of the air masses came over the Atlantic from the SW of Portugal to reach the Canary Islands in the first episode. This is particularly observed in the arrival heights of 1500 and 2700 m, indicating that the bulk of the Saharan aerosols had to move up to these altitudes. In the second episode, the dust plume penetrated further into the Atlantic and required a cyclonic turn to reach the archipelago. The back-trajectories show this behaviour with the air masses turning to reach the islands.

To fully comprehend these episodes, the authors looked at the PM10 (mass concentration in air) from the Copernicus Atmosphere Monitoring Service. Fig. 4 shows the temporal evolution of the two dust episodes (snap images). These images confirm that the aerosols reaching both MLG and TNF belonged to the same dust resuspension events and that the aerosols reaching the TNF monitoring station had been in the atmosphere for over four days when they arrived at this site. This is significant because, in prior studies of dust episodes at the TNF site (Hernández et al., 2005a, 2005b; Karlsson et al., 2008; Stein et al., 2015; López-Pérez et al., 2020), 4-day back-trajectories were used to identify the origin of the aerosol plumes. Thus, the two episodes discussed in this paper would not have been identified as having an African origin. This highlights the importance of combining multidisciplinary data, which provides a more complete picture of the spatial and temporal distribution of air masses.

Hourly variations of PM10 concentration levels near the MLG and

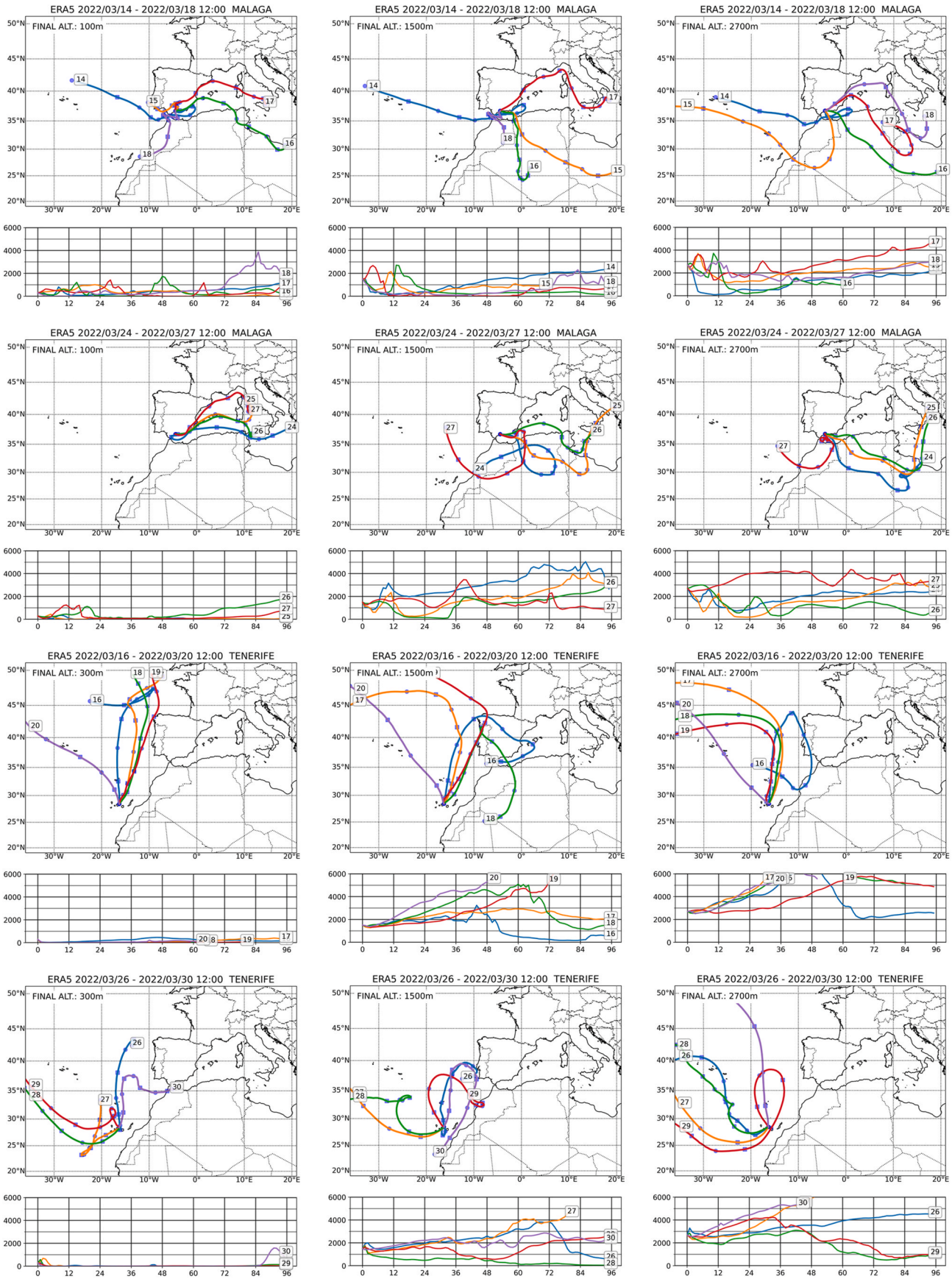

Fig. 3. Four-day HYSPLIT back-trajectories from the monitoring stations in Málaga (MLG) and Tenerife (TNF) during the two dust episodes of March 2022. The altitude of arrival corresponds to the height of the stations (100 m for MLG and 300 m for TNF), 1500 m and 2700 m. The number in the rectangle corresponds to the day of arrival.

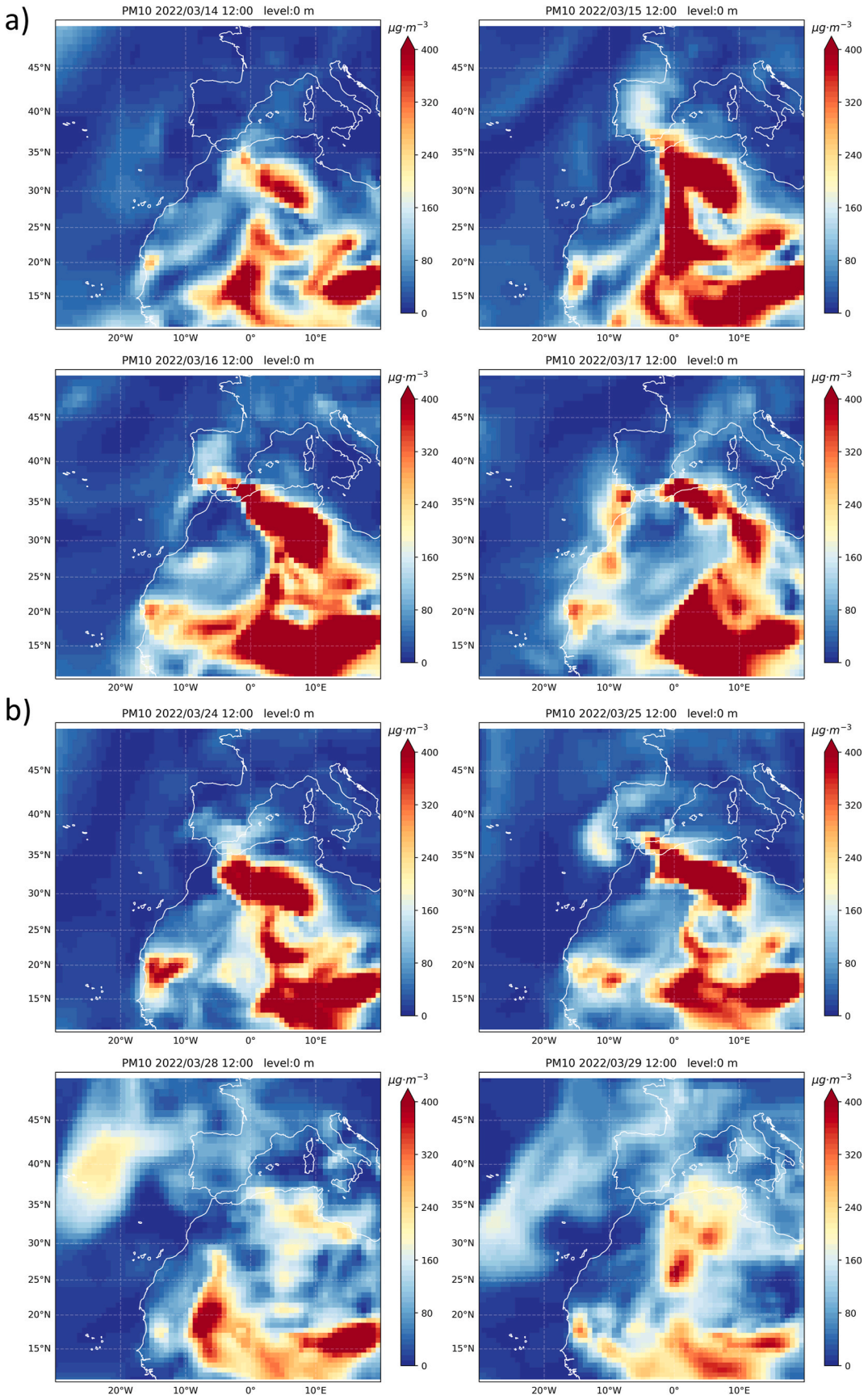

Fig. 4. PM10 aerosol concentrations at the surface a) during the first dust event, 14–17 March 2022; b) for the second dust event, 24–25 and 28–29 March 2022. (Data courtesy of the Copernicus Atmosphere Monitoring Service).

TNF stations are shown in Fig. 5 together with the start and end date of each of the aerosol sample collection periods (see Table S1 in the Supplementary Material). The dashed horizontal line marks the 50 μg m^{-3} limit set by the current European legislation for the concentration of PM10 (See Fig. 5). According to this Air Quality Directive, any given place in the EU cannot exceed an annual average PM10 concentration limit of 40 μg m^{-3}. Moreover, the daily PM10 value (50 μg m^{-3}) cannot be exceeded more than 35 times in a year (EU, 2008). It can be inferred from this figure that the impact of the first Saharan episode in Málaga happened mostly within one aerosol sampling week (MLG-160322) and was most intense within two days (2022-03-14 – 2022-03-16). The second Saharan intrusion at this site was slightly less intense (in terms of peak hourly PM10 concentrations) but lasted longer (2022-03-22 – 2022-03-30). This is why the main radiometric results relevant to this second episode are split into two different samples, the MLG-250322 and the MLG-280322 aerosol samples (lower concentrations were also detected in the following filter sample). The impact of the two Saharan episodes in Tenerife happened within the TFN-210322 and the TFN-040422 aerosol samples, from 2022 to 03-17 – 2022-03-20 and 2022-03-30 – 2022-04-03, respectively. In both cases, as mentioned earlier, the dust material did not travel west from northern Africa (the most common route of dust intrusion to this site). Aerosols were transported instead north towards mainland Spain, and then south towards the Canary Islands as shown in Figs. 3 and 4. This is a significant milestone, since it marks the first occasion where radiometric data have been collected for a dust episode that travelled over both monitoring locations, MLG and then TNF.

As shown in Fig. 5, the Saharan episodes that took place in March 2022 severely impacted the region of Málaga. The maximum hourly PM10 peak concentration recorded was 719 μg m^{-3} for the first episode, and 619 μg m^{-3} for the second one. According to the results, during the sampling periods, the legal daily limit value (50 μg m^{-3}) according to the current European Directive (EU, 2008) was exceeded for eleven days. To put this data into context and comprehend how severe these episodes were, the maximum PM10 concentration reported by (Querol et al., 2019) after analysing the intrusions that reached mainland Spain between 2001 and 2016 was only 320 μg m^{-3}.

Up to 48.7 mm of rainwater was recorded on the 15th and 16th of March at the MLG site (in the first episode), and up to 37.1 mm on the 24th-26th during the second episode. This enhanced the deposition of aerosols from the atmosphere and caused sharp drops in hourly PM10 concentrations. Radionuclide content in the rainwater collected during these two episodes is provided further below (see Table 1). In contrast, the maximum hourly PM10 concentration recorded in Tenerife during the period of interest was 298 μg m^{-3} (compared to the maximum ever recorded at this site of 3000 μg m^{-3} in February 2020 (López-Pérez

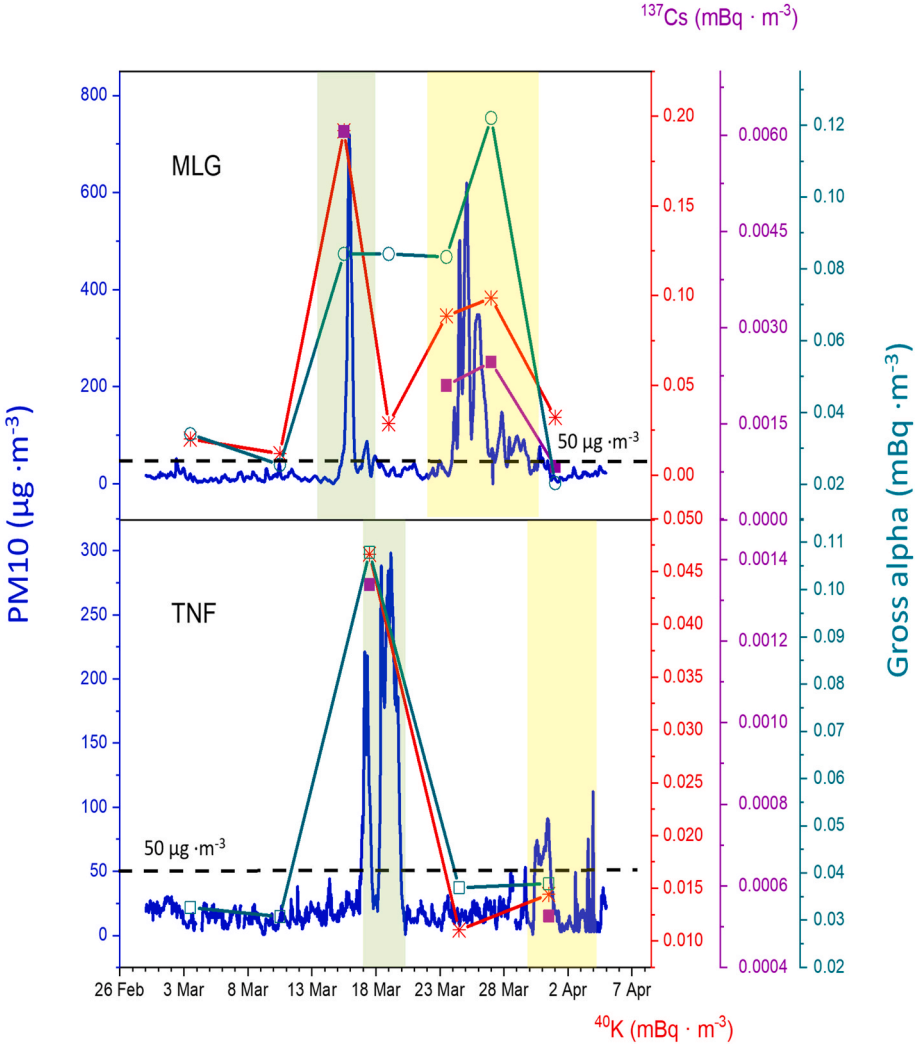

Fig. 5. Hourly levels of PM10 in March 2022. The dashed horizontal line of 50 μg m^{-3} marks the limit set by the current European legislation for the concentration of PM10 (EU, 2008). Activity concentrations of ^{40}K, ^{137}Cs and gross alpha concentrations in surface-level aerosols measured at MLG and TNF monitoring stations during March 2022. Shady areas mark when the episodes reached each of the monitoring sites.

Table 1
Radionuclide concentrations in rainwater deposits collected at the MLG monitoring station after the two dust events that took place in March 2022, and calculated deposition rates.

		^{7}Be		^{40}K		^{137}Cs		^{210}Pb		^{7}Be/^{210}Pb		^{137}Cs/^{40}K	
SAMPLE		Value	Unc	Value	Unc	Value	Unc	Value	Unc	Value	Unc	Value	Unc
MLG-WD-160322	**Activity concentration** (Bq m^{-3})	66E+2	4E+2	23E+2	2E+2	5E+1	1E+1	22E+2	3E+2	29E-1	4E-1	21E-3	5E-3
March 15–16th	**Deposition** (Bq m^{-2})	64E+1	3E+1	22E+1	2E+1	5E+0	1E+0	22E+1	3E+1	29E-2	4E-2	20E-4	5E-4
48.7 mm	**Deposition Flux** (Bq m^{-2} d^{-1})	56E+1	3E+1	20E+1	2E+1	42E-1	9E-1	19E+1	2E+1	25E-2	4E-2	18E-4	4E-4
MLG-WD-250322	**Activity concentration** (Bq m^{-3})	142E+2	8E+2	104E+2	8E+2	19E+1	3E+1	60E+2	8E+2	24E-1	4E-1	18E-3	3E-3
March 24–25th	**Deposition** (Bq m^{-2})	53E+1	3E+1	39E+1	3E+1	7E+0	1E+0	22E+1	3E+1	9E-2	1E-2	7E-4	1-E4
37.1 mm	**Deposition Flux** (Bq m^{-2} d^{-1})	43E+1	3E+1	32E+1	2E+1	58E-1	9E+1	18E+1	2E+1	7E-2	1E-2	6E-4	1E-4

et al., 2020). No rainfall samples were collected at the TNF station during these events.

3.2. Levels of radionuclides in aerosol samples

Table S1 in the Supplementary Material shows the concentration of radionuclides (^{7}Be, ^{210}Pb, ^{40}K, ^{137}Cs), gross alpha and gross beta activity measured in the aerosol filters during the period of interest (2022-02-28 – 2022-04-04) at the MLG and TNF radiological monitoring stations. The total number of HVS aerosol samples collected at the MLG station was 7, and 5 at the TNF station. The MLG station had to subdivide their standard weekly sampling during the two weeks of intense Saharan episodes to prevent total saturation of the HVS filters. This was not necessary at the TNF site since the concentrations of aerosols (PM10) recorded during these Saharan episodes were approximately half of those documented in Málaga. Fig. 5 shows when the two episodes reached each of the monitoring sites. The number of LVS samples for gross alpha and gross beta activities was six for the MLG station and five for the TFN station. The TSP values shown in Table S1 in the Supplementary Material were calculated by dividing the total mass of aerosols collected in each filter by the volume of air sampled. Although other short-lived radionuclides from the natural series were also detected via gamma spectrometry in the aerosol filters, they are not presented herein since the data is not representative of the complete sampling period.

In terms of TSP for the HVS sampler, the maximum values recorded at the MLG station were 382 and 185 μg m^{-3} during the first and second episode, respectively, and 83 μg m^{-3} and 37 μg m^{-3} at the TNF station. Average TSP concentration during these Saharan dust episodes was higher at the MLG station by more than one order of magnitude compared to the yearly mean value of 40 μg m^{-3} for the period 2009–2011 (Gordo et al., 2015b).

To put the radiometric intensity of the episodes examined in this work into context, it is important to note that before the Saharan events discussed here, the monitoring station in Málaga had consistently recorded ^{137}Cs concentrations in aerosol samples that fell below the minimum detectable activity. This station has been operational with an HVS sampler since 2009. Thus, this is the most intense set of dust intrusions since the station started collecting data with the HVS. The monitoring station in Tenerife has recorded, since 2000, over ninety Saharan intrusions. The maximum ^{137}Cs concentration ever recorded at this station related to a Saharan episode was 11.7 ± 0.1 μBq·m^{-3}, in March 2004 (Hernández et al., 2005a). This is, after decay correction, approximately the same concentration reported here for Málaga, and seven times higher than the concentration reported here for Tenerife during this period.

In terms of ^{40}K, the maximum concentration ever documented by the MLG monitoring station was during the first of the two Saharan episodes studied here, with a value close to 200 μBq·m^{-3}. The highest ^{40}K concentration in the Tenerife station during the period of interest was 47 ± 3 μBq·m^{-3}. This is approximately three times lower than the maximum concentration ever reported at this sampling site, 165 ± 4 μBq·m^{-3}, which was during an extreme winter Saharan episode in February 2020 (López-Pérez et al., 2020).

In terms of gross alpha activities, the maximum value in MLG was detected during the second Saharan event, even though the hourly peak PM10 concentrations were not as high as during the first episode. The alpha emitter ^{210}Po, a descendent of ^{210}Pb, is often the main contributor to the gross alpha activities in the atmosphere (Terray et al., 2020). However, it has also been shown that gross alpha activities normally underestimate the concentrations of ^{210}Po due to alpha particle attenuation (Terray et al., 2020). This may explain why higher PM10 concentrations in the first dust intrusion in MLG did not result in the highest gross alpha activities. In comparison with previous recordings, the gross alpha activities reported for these two events were not the highest at this site, 84 ± 7 μBq·m^{-3} for the first episode and 112 ± 12 μBq·m^{-3} for the second episode. In the case of the TNF site, the gross alpha activities determined in February 2020 were approximately sixteen times higher than the maximum reported for the March 2022 period (López-Pérez et al., 2020).

It has been suggested that gross beta activity from LVS samplers can be used as a good indicator of the evolution of ^{210}Pb concentration in the air (Duch et al., 2016). About 61–87 % of the gross beta activity comes from ^{210}Pb (Dueñas et al., 2004; Huang et al., 2009). The impact of Saharan episodes on ^{210}Pb, ^{7}Be and gross beta concentrations in aerosol samples is more complex and most likely depends on the altitude at which the Saharan aerosols are resuspended and transported in the atmosphere (Hernandez et al., 2007, 2008; Gordo et al., 2015b; Zalewska and Biernacik, 2022).

The radiometric results of the first sample at each station shown in Fig. 5 represent the background conditions usually observed at these locations. The results for the subsequent samples show that the Saharan dust episodes produced a pronounced increase in the concentration of aerosol particles and radionuclides activities (^{40}K, ^{137}Cs and gross alpha) compared to the background conditions at these two sites. However, not all radionuclides were impacted in the same way. As previously reported, increases in ^{137}Cs, ^{40}K, gross alpha, PM10 and TSP concentrations are usually correlated with Saharan episodes (Hernández et al., 2005a; Karlsson et al., 2008; López-Pérez et al., 2020). Such an increase, particularly in ^{137}Cs, during Saharan episodes, has also been reported in Monaco (Pham et al., 2005, 2017, 2020) and in France (Menut et al., 2009; Masson et al., 2010).

Fig. 5 shows that the concentrations of ^{137}Cs and ^{40}K correlate well with the peaks of hourly PM10 concentrations. A very good agreement was also observed in the temporal evolution of the gross alpha activity and peak PM10 data from the TNF station. However, the same relationship between gross alpha activity and peak PM10 is not evident for

the MLG data (see 4th, 5th and 6th data points in Fig. 5). The authors believe this could be related to the presence of ^{222}Rn and ^{210}Po in the air (both alpha emitters), also transported from the north of Africa during these events. ^{222}Rn gas may have remained in the atmosphere over MLG even after the main dust plume had passed the area and cleared particulate matter, especially since ^{222}Rn gas is less affected by rain. Nonetheless, this will require further research.

Fig. 6 shows the concentrations, in mBq·g^{-1}, of ^{137}Cs and ^{40}K recorded at the two monitoring stations during these episodes. The ^{137}Cs concentrations recorded for the first and second dust episodes agree surprisingly well: ~15 ± 2 mBq·g^{-1}, even though the aerosols were airborne for over three days between these two monitoring stations. This is perhaps not surprising for ^{137}Cs, which is often associated with small-size aerosols that can have long atmospheric residence times (López-Pérez et al., 2013). The authors believe that the ^{137}Cs data in Fig. 6 show that the source of the dust for both events in March 2022 originated in the same region in Africa and the small variations in the data are related to the long aerosol sampling times used in this study. This result is in agreement with the data shown in Fig. 4.

The concentrations of ^{40}K shown in Fig. 6 ranged between 200 and 600 mBq·g^{-1}. All concentrations recorded during dust intrusions (highlighted in green and yellow) were above 400 mBq·g^{-1} at the MLG station and 350 mBq·g^{-1} at the TFN station. However, the first and second data points for the MLG-station (MLG-070322 and MLG-140322) were also above 400 mBq·g^{-1} and cannot be directly correlated to a dust intrusion (or peak of PM10 particles in the atmosphere). This indicates that there is at least another source of this nuclide at this site. This is confirmed by the fact that this radionuclide has been often detected at this site since the monitoring started (unlike ^{137}Cs). This additional source is most likely continental because of the location of this site. This is not the case for the TNF-station where ^{40}K is almost always associated with dust intrusions. The ratio ^{40}K to ^{137}Cs, for the samples where ^{137}Cs was detected (i.e., dust related), were found to be around 35 ± 5, which is a relatively narrow band, especially when data from two different sites are compared. Further statistical analysis using long-time series will be needed to establish the true significance of this ratio and its utility for tracer studies.

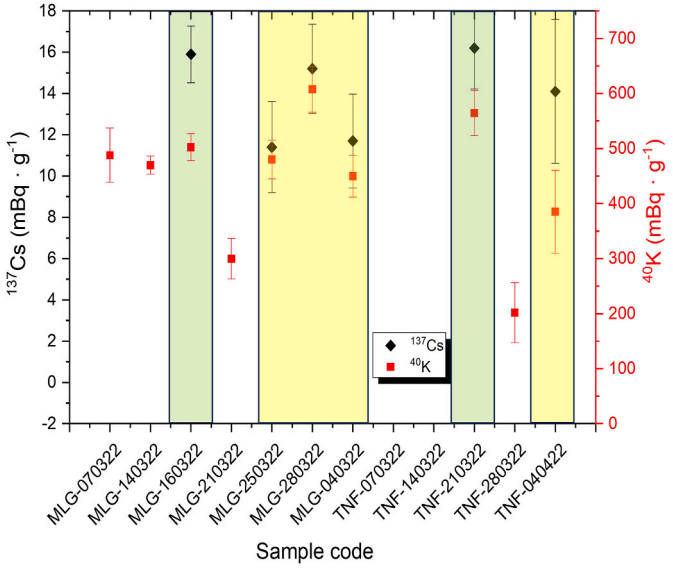

Fig. 6. ^{40}K (*squares*) and ^{137}Cs (*diamonds*) concentrations (in mBq·g^{-1}) measured in the aerosol samples collected at the MLG and TNF monitoring stations during the period of interest. Green and yellow shaded areas represent the first and second periods with dust intrusion (for details see Fig. 5).

3.3. Isotopic ratios

^{137}Cs, ^{239}Pu and ^{240}Pu ratios can be calculated and compared to identify the origin of these radionuclides (Masson et al., 2005). A ^{240}Pu/^{239}Pu ratio of approximately 0.18 and ^{137}Cs/$^{239+240}$Pu < 40 means the origin of the plutonium isotopes is due to global fallout. A ratio of ^{137}Cs/$^{239+240}$Pu greater than 40 means that an additional source of ^{137}Cs other than global fallout is involved (Brandt et al., 2002; Masson et al., 2005; Kulan, 2006). Table S2 in the Supplementary Material shows ^{240}Pu/^{239}Pu and ^{137}Cs (decay corrected to 1998)/$^{239+240}$Pu ratios measured in four aerosol samples collected from both monitoring stations. Plutonium isotopes were only determined in two samples from each of the sampling sites. The ^{240}Pu/^{239}Pu ratios, close to 0.18 confirm that the source of the plutonium isotopes measured on these filters is from global weapons fallout, i.e., there are no signs that plutonium from the French nuclear weapon tests performed in Algeria in the 60s contributed in any way to the presence of these isotopes in the aerosols transported in the two dust events studied here. The ratios between ^{137}Cs (decay corrected to 1998) and $^{239+240}$Pu, close to 44, indicate that there is an excess of ^{137}Cs which is not related to the global weapons fallout. The expected ratio for global weapons fallout for this region would be around 20 (Baggoura et al., 1998). It is likely that ^{137}Cs deposited over northern Africa after the Chernobyl NPP accident explains the higher ratios recorded in the aerosol samples (López-Pérez et al., 2022).

3.4. Levels of radionuclides in wet deposition samples

Table 1 shows the concentrations of the gamma-emitting radionuclides measured in the rainwater samples collected at the MLG monitoring station during the two dust episodes in March 2022. This is the first time that individual radiological investigations of the wet fraction of high-deposition Saharan dust episodes collected at this sampling location have been reported. Unfortunately, no rainwater was collected at the monitoring station in Tenerife during these two events to allow a comparison between the two locations. Although the peak PM10 concentrations at the surface level in Málaga and the amount of rain collected were higher during the first dust event, the concentrations of both ^{137}Cs and ^{40}K in the rainwater deposited were greater during the second one. One of the causes could be the variations of PM10 concentrations with altitude, but there are other variables affecting wet deposition processes that may have influenced the radiometric data obtained here.

Table 1 also presents the deposition fluxes for individual radionuclides in terms of activity per area (Bq·m^{-2}) as well as time (Bq·m^{-2}·d^{-1}) assuming 24 h of rain. Depositional fluxes of three natural radionuclides ^{7}Be, ^{210}Pb, ^{40}K collected on a monthly basis in the period 2005–2015 were reported for Málaga (Dueñas et al., 2017). The average annual depositions were 1215 Bq·m^{-2}·year^{-1}, 144 Bq·m^{-2}·year^{-1} and 67 Bq·m^{-2}·year^{-1} (Dueñas et al., 2017), respectively, with the highest ^{40}K flux occurring in October 2008 due to an intense African dust outbreak (Cabello et al., 2012). In comparison, the data from the two massive episodes in March 2022 corresponded to approximately 1/3 of the expected annual flux for ^{7}Be, exceeding the combined yearly contribution of both ^{210}Pb and ^{40}K. Associated with particulate matter deposition, unusual ^{137}Cs concentrations were found in rainwater samples collected in Málaga. Compared to other sites, a peak of ^{137}Cs in a deposition rate of 29.7 mBq·m^{-2}·d^{-1} during the large-scale Asian dust events was reported in northern Japan, occurring from March 7 to March 25, 2002 (Akata et al., 2007). The data obtained in the present study, 2–5 Bq·m^{-2}·d^{-1}, is almost two orders of magnitude higher than those reported in Japan. The ^{137}Cs deposition in Monaco reported by (Pham et al., 2017) from the Saharan dust event in February 2004 was 0.79 Bq·m^{-2}. ^{137}Cs levels in dust deposition collected in several locations in France during the same exceptional dust outbreak were in the range of 0.4–1.3 Bq·m^{-2} (Masson et al., 2010). The high particle flux, combined with trace levels of ^{137}Cs

in these particles, causes a radionuclide flux that corresponds to major transportation events of radionuclides from one place to another, contributing to the current background level of artificial radionuclides at trace levels in the atmosphere (Masson et al., 2010).

Wet deposition during dust outbreaks is typically known as "red rain", "dust rain", "blood rain", or "muddy rain" (Sala et al., 1996; Avila et al., 1997; Fiol et al., 2005; White et al., 2012). In some cases, these events are considered extreme, with 10–40 g m^{-2} of dust deposited after a single red rain event. Several intense wintertime dust deposition events have been recorded in Europe in recent years. These unusual episodes were characterised by severe washout of mineral dust material and were related to highly similar synoptic meteorological situations (Varga, 2020). For example, an average of 18 ± 8 g m^{-2} wet deposition of dust was reported for the city of Granada (south Iberian Peninsula) during an event in February 2017 (Rodriguez-Navarro et al., 2018). These values exceeded the annual average of Saharan dust dry deposition in south-western Europe, which was estimated to range from approximately 3 to 14 g m^{-2} (Goudie and Middleton, 2001).

Using the activity concentrations (in Bq·g^{-1}) reported in Fig. 6, the amount of atmospheric aerosols deposited by rain (wet deposition) was calculated for the two events, based on both the ^{137}Cs and the ^{40}K concentrations, which are known to be mainly associated with Saharan dust intrusions. The results for the first rain event (March 14–15th) were 16 ± 4 g m^{-2} of aerosols (based on ^{137}Cs data) and 24 ± 3 g m^{-2} of aerosols (based on ^{40}K data). Estimates for the wet deposition during the second dust event (March 24–25th) were 33 ± 6 g m^{-2} of aerosols (^{137}Cs) and 43 ± 4 g m^{-2} (^{40}K). Thus, the data obtained agrees well with both rain events. In addition, these values were similar to those reported for the Granada episode of 2017 (10–40 g m^{-2}) and much higher than the yearly average for the region. Assuming that the rain events in Málaga lasted for 24 h in each case, the wet deposition rates would range between 660 and 1400 mg m^{-2}·h^{-1}. Studies of dust deposition flux measurements in Gran Canaria (Canary Islands) estimated that the main contribution to the annual particle fluxes is from dust inputs occurring during periods of African dust transport (Gelado-Caballero et al., 2012). Dry deposition dominated the particle fluxes and an average value of 25.0 ± 0.3 mg m^{-2}·d^{-1} was measured during a three-year time-series measurement (López-García et al., 2013). This means that the wet deposition estimate would be equivalent to approximately 26–56 days of dry deposition in Gran Canaria, which highlights the importance that wet deposition has on the atmospheric deposition of dust aerosols during outbreaks.

4. Conclusions

Two intense Saharan dust episodes that impacted southern Europe and the Canary Islands in March 2022 have been studied in this work. The mechanics of both events were similar. These two extreme episodes significantly increased the concentrations of PM10, ^{137}Cs, ^{40}K and gross alpha activities in atmospheric aerosols monitored at two different locations: MLG (southern mainland Spain) and TNF (Canary Islands). While similar increases have been previously reported at the TNF monitoring station as a result of other Saharan dust intrusions, this is the first time, since the start of operations at the MLG monitoring station, that such increases, especially in ^{137}Cs concentrations, are reported.

The intensity of the dust episodes was higher in MLG compared to TNF because the aerosols travelled first in a northwest direction over this site before veering south toward the Canary Islands. Most radiometric data previously presented by the TNF station regarding dust intrusions are the result of direct transport of dust from northern Africa in a westerly direction over the islands. However, the data presented here showed how Saharan aerosols remained in the atmosphere for 4–5 days over the Atlantic and reached this site from the north/north-west. This suggests that prior findings which relied on 4-day back-trajectories and categorised air masses into two groups - African and Atlantic origin - may require a reassessment for reasons of accuracy. There may have been occasions where concentrations of ^{137}Cs and ^{40}K were caused by Saharan aerosols even though the air masses were classified as Atlantic.

The ^{137}Cs concentrations, in Bq·g^{-1} of aerosol, measured at both sites indicate that both events in March 2022 had the same source of aerosols. The ^{40}K concentrations, in Bq·g^{-1}, showed that the MLG station has a second source of ^{40}K, most likely related to its location in continental Europe, which is not observed in TFN station.

The ^{240}Pu and ^{239}Pu ratios measured for some of the aerosol filters collected during these episodes indicate that the source of these isotopes was global atmospheric fallout from weapon tests. However, the ratios between ^{137}Cs and $^{239+240}$Pu suggest that there are additional sources of ^{137}Cs. Based on the values, the authors believe there were also ^{137}Cs from the Chernobyl NPP accident previously deposited over the north of Africa.

^{137}Cs and ^{40}K concentrations measured in rainwater collected at the MLG station during the two dust episodes showed how effective rain was at "cleaning the air" (decreasing the concentration of PM10 particles by one order of magnitude) at this site. It was estimated that the rain enhanced the deposition of aerosols to an equivalent of 26–56 days of dry deposition.

The results reported in the present study provide additional insights into the dependence of the particle properties on source regions, and on the geographical location where they are collected. These may be of value to the scientific community since they contribute to documenting and understanding the interaction between mineral aerosols and the environment.

Even though the cases studied here lasted a few days, the radiological impact reported here suggests that this type of extreme dust event from the Sahara could have strong regional implications. In addition, the information gathered implies an ongoing enrichment process of ^{137}Cs and plutonium isotopes in the soils of receptor areas, a consequence of the resuspension, transport, and deposition of Saharan dust.

The concentrations of radionuclides detected in the analysed aerosol samples do not pose any radiological risk to the population.

CRediT authorship contribution statement

Esperanza Liger: Writing – review & editing, Writing – original draft, Formal analysis, Data curation, Conceptualization. **Francisco Hernández:** Writing – review & editing, Writing – original draft, Formal analysis, Data curation, Conceptualization. **Francisco Javier Expósito:** Formal analysis, Software, Visualization, Writing – review & editing. **Juan Pedro Díaz:** Formal analysis, Software, Visualization, Writing – review & editing. **Pedro A. Salazar-Carballo:** Formal analysis, Visualization, Writing – review & editing. **Elisa Gordo:** Writing – review & editing, Visualization, Investigation, Data curation. **Cristina González:** Writing – review & editing, Visualization, Data curation. **María López-Pérez:** Writing – review & editing, Visualization, Investigation, Data curation.

Declaration of competing interest

The authors declare that they have no known competing financial interests or personal relationships that could have appeared to influence the work reported in this paper.

Data availability

Data will be made available on request.

Acknowledgments

This work has been partially supported by the Spanish Nuclear Safety Council (CSN). The authors would like to thank Gabriel Castelló Ortega from the Central Research Facilities at the University of Malaga for his technical assistance. The authors gratefully acknowledge the NOAA Air

Resources Laboratory (ARL) for the provision of the HYSPLIT transport and dispersion model and/or READY website (https://www.ready.noaa.gov) used in this publication. The authors gratefully acknowledge the use of imagery from the Copernicus Atmosphere Monitoring Service (https://ads.atmosphere.copernicus.eu/). The authors also acknowledge the use of imagery from the Worldview Snapshots application https://wvs.earthdata.nasa.gov), part of the Earth Observing System Data and Information System (EOSDIS). The authors also appreciate the support of the Government of the Canary Islands, the Ministry of Ecological Transition, Fight against Climate Change and Territorial Planning (agreement published: B.O.C. no. 238, November 20, 2020) and the PLANCLIMAC Project (MAC/3.5b/244). This Project has been funded by the INTERREG MAC 2014–2020 Program of the European Union. Funding for open access charge: University of Málaga / CBUA..

Appendix A. Supplementary data

Supplementary data to this article can be found online at https://doi.org/10.1016/j.chemosphere.2024.141303.

References

Aba, A., Al-Dousari, A.M., Ismaeel, A., 2018. Atmospheric deposition fluxes of 137Cs associated with dust fallout in the northeastern Arabian Gulf. J. Environ. Radioact. 192, 565–572I. https://doi.org/10.1016/j.jenvrad.2018.05.010.

AEMET, 2022. Informe acerca de la intrusión de polvo de origen sahariano sobre el territorio peninsular español entre los días 14 y 16 de marzo de 2022.

AEMET, 2023. Informe anual 2022, Ministerio para la Transición Ecológica y el Reto Demográfico, ed. Madrid.

Akata, N., Hasegawa, H., Kawabata, H., Chikuchi, Y., Sato, T., Ohtsuka, Y., Kondo, K., Hisamatsu, S., 2007. Deposition of 137Cs in Rokkasho, Japan and its relation to Asian dust. J. Environ. Radioact. 95, 1–9I. https://doi.org/10.1016/j.jenvrad.2007.01.007.

Alonso-Pérez, S., Cuevas, E., Querol, X., Viana, M., Guerra, J.C., 2007. Impact of the Saharan dust outbreaks on the ambient levels of total suspended particles (TSP) in the marine boundary layer (MBL) of the Subtropical Eastern North Atlantic Ocean. Atmos. Environ. 41, 9468–9480I. https://doi.org/10.1016/j.atmosenv.2007.08.049.

Alonso-Pérez, S., Cuevas, E., Querol, X., 2011. Objective identification of synoptic meteorological patterns favouring African dust intrusions into the marine boundary layer of the subtropical eastern north Atlantic region. Meteorol. Atmos. Phys. 113, 109–124I. https://doi.org/10.1007/s00703-011-0150-z.

Amato, F., Alastuey, A., de la Rosa, J., Gonzalez Castanedo, Y., Sánchez de la Campa, A. M., Pandolfi, M., Lozano, A., Contreras González, J., Querol, X., 2014. Trends of road dust emissions contributions on ambient air particulate levels at rural, urban and industrial sites in southern Spain. Atmos. Chem. Phys. 14, 3533–3544I. https://doi.org/10.5194/acp-14-3533-2014.

Arimoto, R., Ray, B.J., Lewis, N.F., Tomza, U., Duce, R.A., 1997. Mass-particle size distributions of atmospheric dust and the dry deposition of dust to the remote ocean. J. Geophys. Res. Atmos. 102, 15867–15874I. https://doi.org/10.1029/97JD00796.

Avila, A., Queralt-Mitjans, I., Alarcón, M., 1997. Mineralogical composition of African dust delivered by red rains over northeastern Spain. J. Geophys. Res. Atmos. 102, 21977–21996I. https://doi.org/10.1029/97JD00485.

Baggoura, B., Noureddine, A., Benkrid, M., 1998. Level of natural and artificial radioactivity in Algeria. Appl. Radiat. Isot. 49, 867–873I. https://doi.org/10.1016/S0969-8043(97)10005-7.

Barbosa, P., Guimarães-Pereira, Â., Hernández-González, Y., Cuevas, E., Rodríguez, S., 2016. Perspectives on Contentions about Climate Change Adaptation in the Canary Islands – A Case Study for Tenerife. European Commission, Joint Research Centre. Publications Office.

Barreto, Á., Cuevas, E., García, R.D., Carrillo, J., Prospero, J.M., Ilić, L., Basart, S., Berjón, A.J., Marrero, C.L., Hernández, Y., Bustos, J.J., Ničković, S., Yela, M., 2022. Long-term characterisation of the vertical structure of the Saharan Air Layer over the Canary Islands using lidar and radiosonde profiles: implications for radiative and cloud processes over the subtropical Atlantic Ocean. Atmos. Chem. Phys. 22, 739–763I. https://doi.org/10.5194/acp-22-739-2022.

Brandt, J., Christensen, J.H., Frohn, L.M., 2002. Modelling transport and deposition of caesium and iodine from the Chernobyl accident using the DREAM model. Atmos. Chem. Phys. 2, 397–417I. https://doi.org/10.5194/acp-2-397-2002.

C3S, ERA5: Fifth Generation of ECMWF Atmospheric Reanalyses of the Global Climate. Copernicus Climate Change Service, Climate Data Store (CDS). https://cds.climate.copernicus.eu/cdsapp#!/home.

Cabello, M., Orza, J.A.G., Barrero, M.A., Gordo, E., Berasaluce, A., Cantón, L., Dueñas, C., Fernández, M.C., Pérez, M., 2012. Spatial and temporal variation of the impact of an extreme Saharan dust event. J. Geophys. Res. Atmos. 117 https://doi.org/10.1029/2012JD017513.

Cachorro, V.E., Burgos, M.A., Mateos, D., Toledano, C., Bennouna, Y., Torres, B., de Frutos, Á.M., Herguedas, Á., 2016. Inventory of African desert dust events in the north-central Iberian Peninsula in 2003–2014 based on sun-photometer–AERONET and particulate-mass–EMEP data. Atmos. Chem. Phys. 16, 8227–8248I. https://doi.org/10.5194/acp-16-8227-2016.

Çapraz, Ö., Deniz, A., 2021. Particulate matter (PM10 and PM2.5) concentrations during a Saharan dust episode in Istanbul. Air Quality, Atmosphere & Health 14, 109–116I. https://doi.org/10.1007/s11869-020-00917-4.

AEMET, Borrasca Celia. https://www.aemet.es/es/conocermas/borrascas/2021-2022/estudios_e_impactos/celia.

Chamizo, E., Jiménez-Ramos, M.C., Wacker, L., Vioque, I., Calleja, A., García-León, M., García-Tenorio, R., 2008. Isolation of Pu-isotopes from environmental samples using ion chromatography for accelerator mass spectrometry and alpha spectrometry. Anal. Chim. Acta 606, 239–245I. https://doi.org/10.1016/j.aca.2007.11.005.

Chamizo, E., Christl, M., Fifield, L.K., 2015. Measurement of 236U on the 1MV AMS system at the Centro Nacional de Aceleradores (CNA). Nucl. Instrum. Methods Phys. Res. Sect. B Beam Interact. Mater. Atoms 358, 45–51I. https://doi.org/10.1016/j.nimb.2015.05.008.

Chiapello, I., Bergametti, G., Gomes, L., Chatenet, B., Dulac, F., Pimenta, J., Suares, E.S., 1995. An additional low layer transport of Sahelian and Saharan dust over the north-eastern Tropical Atlantic. Geophys. Res. Lett. 22, 3191–3194I. https://doi.org/10.1029/95GL03313.

COPERNICUS, Atmosphere Data Store. https://ads.atmosphere.copernicus.eu/#!/home.

Copernicus. "Historic" Saharan dust episode in western Europe – CAMS predictions accurate, https://atmosphere.copernicus.eu/historical-saharan-dust-episode-western-europe-cams-predictions-accurate.

Csn, Red de vigilancia de ámbito nacional (REVIRA). https://www.csn.es/ca/red-de-vigilancia-radiologica-de-ambito-nacional-revira.

Cuevas, E., Milford, C., Barreto, A., Bustos, J.J., García, R.D., Marrero, C.L., Prats, N., Bayo, C., Ramos, R., Terradellas, E., Suárez, D., Rodríguez, S., de la Rosa, J., Vilches, J., Basart, S., Werner, E., López-Villarrubia, E., Rodríguez-Mireles, S., Pita Toledo, M.L., González, O., Belmonte, J., Puigdemunt, R., Lorenzo, J.A., Oromí, P., del Campo-Hernández, R., 2021. Desert dust outbreak in the canary islands (February 2020): Assessment and impacts. In: Cuevas, E., Milford, C., Basart, S. (Eds.), State Meteorological Agency (AEMET), WMO Global Atmosphere Watch (GAW) Report. Madrid, Spain and World Meteorological Organization, Geneva, Switzerland. No. 259, WWRP 2021-1.

de la Rosa, J.D., Sánchez de la Campa, A.M., Alastuey, A., Querol, X., González-Castanedo, Y., Fernández-Camacho, R., Stein, A.F., 2010. Using PM10 geochemical maps for defining the origin of atmospheric pollution in Andalusia (Southern Spain). Atmos. Environ. 44, 4595–4605I. https://doi.org/10.1016/j.atmosenv.2010.08.009.

Díaz, J., Linares, C., Carmona, R., Russo, A., Ortiz, C., Salvador, P., Trigo, R.M., 2017. Saharan dust intrusions in Spain: health impacts and associated synoptic conditions. Environ. Res. 156, 455–467I. https://doi.org/10.1016/j.envres.2017.03.047.

Duch, M.A., Serrano, I., Cabello, V., Camacho, A., 2016. Comparison of different sampling methods for the determination of low-level radionuclides in air. Appl. Radiat. Isot. 109, 456–459I. https://doi.org/10.1016/j.apradiso.2015.11.042.

Dueñas, C., Fernández, M.C., Liger, E., Carretero, J., 1999. Gross alpha, gross beta activities and 7Be concentrations in surface air: analysis of their variations and prediction model. Atmos. Environ. 33, 3705–3715I. https://doi.org/10.1016/S1352-2310(99)00172-7.

Dueñas, C., Fernández, M.C., Carretero, J., Liger, E., Cañete, S., 2001. Gross-alpha and gross-beta activities in airborne particulate samples. Analysis and prediction models. Appl. Radiat. Isot. : including data, instrumentation and methods for use in agriculture, industry and medicine 54, 645–654I. https://doi.org/10.1016/S0969-8043(00)00298-0.

Dueñas, C., Fernández, M.C., Carretero, J., Liger, E., Cañete, S., 2004. Long-term variation of the concentrations of long-lived Rn descendants and cosmogenic 7Be and determination of the MRT of aerosols. Atmos. Environ. 38, 1291–1301I. https://doi.org/10.1016/j.atmosenv.2003.11.029.

Dueñas, C., Gordo, E., Liger, E., Cabello, M., Cañete, S., Pérez, M., Torre-Luque, P.d.l., 2017. 7Be, 210Pb and 40K depositions over 11 years in Málaga. J. Environ. Radioact. 178–179, 325–334I. https://doi.org/10.1016/j.jenvrad.2017.09.010.

Engelstaedter, S., Tegen, I., Washington, R., 2006. North African dust emissions and transport. Earth Sci. Rev. 79, 73–100I. https://doi.org/10.1016/j.earscirev.2006.06.004.

Escudero, M., Castillo, S., Querol, X., Avila, A., Alarcón, M., Viana, M.M., Alastuey, A., Cuevas, E., Rodríguez, S., 2005. Wet and dry African dust episodes over eastern Spain. J. Geophys. Res. Atmos. 110 https://doi.org/10.1029/2004JD004731.

Escudero, M., Querol, X., Pey, J., Alastuey, A., Pérez, N., Ferreira, F., Alonso, S., Rodríguez, S., Cuevas, E., 2007. A methodology for the quantification of the net African dust load in air quality monitoring networks. Atmos. Environ. 41, 5516–5524I. https://doi.org/10.1016/j.atmosenv.2007.04.047.

EU, 2008. Directive 2008/50/EC of the European Parliament and of the Council of 21 May 2008 on ambient air quality and cleaner air for Europe. Orkesterjournalen L 152, 1–44, 11.6.2008.

Eyrolle, F., Masson, O., Antonelli, C., Arnaud, M., Charmasson, S., 2009. The EXTREME project consequences of paroxystic meteo climatic events on the translocation of contaminants within the geosphere. Radioprotection 44, 463–468I. https://doi.org/10.1051/radiopro/20095086.

Fernández, A.J., Sicard, M., Costa, M.J., Guerrero-Rascado, J.L., Gómez-Amo, J.L., Molero, F., Barragán, R., Basart, S., Bortoli, D., Bedoya-Velásquez, A.E., Utrillas, M. P., Salvador, P., Granados-Muñoz, M.J., Potes, M., Ortiz-Amezcua, P., Martínez-Lozano, J.A., Artíñano, B., Muñoz-Porcar, C., Salgado, R., Román, R., Rocadenbosch, F., Salgueiro, V., Benavent-Oltra, J.A., Rodríguez-Gómez, A., Alados-Arboledas, L., Comerón, A., Pujadas, M., 2019. Extreme, wintertime Saharan dust intrusion in the Iberian Peninsula: lidar monitoring and evaluation of dust forecast models during the February 2017 event. Atmos. Res. 228, 223–241I. https://doi.org/10.1016/j.atmosres.2019.06.007.

Fiol, L.A., Fornós, J.J., Gelabert, B., Guijarro, J.A., 2005. Dust rains in Mallorca (Western Mediterranean): their occurrence and role in some recent geological processes. Catena 63, 64–84I. https://doi.org/10.1016/j.catena.2005.06.012.

Fujiwara, H., 2016. Observation of radioactive iodine (131I, 129I) in cropland soil after the Fukushima nuclear accident. Sci. Total Environ. 566–567, 1432–1439I. https://doi.org/10.1016/j.scitotenv.2016.06.004.

Gelado-Caballero, M.D., López-García, P., Prieto, S., Patey, M.D., Collado, C., Hérnández-Brito, J.J., 2012. Long-term aerosol measurements in Gran Canaria, Canary Islands: particle concentration, sources and elemental composition. J. Geophys. Res. Atmos. 117 https://doi.org/10.1029/2011JD016646.

Gelaro, R., McCarty, W., Suárez, M.J., Todling, R., Molod, A., Takacs, L., Randles, C.A., Darmenov, A., Bosilovich, M.G., Reichle, R., Wargan, K., Coy, L., Cullather, R., Draper, C., Akella, S., Buchard, V., Conaty, A., da Silva, A.M., Gu, W., Kim, G.-K., Koster, R., Lucchesi, R., Merkova, D., Nielsen, J.E., Partyka, G., Pawson, S., Putman, W., Rienecker, M., Schubert, S.D., Sienkiewicz, M., Zhao, B., 2017. The Modern-Era Retrospective analysis for research and applications, Version 2 (MERRA-2). J. Clim. 30, 5419–5454I. https://doi.org/10.1175/JCLI-D-16-0758.1.

Gerasopoulos, E., Kouvarakis, G., Babasakalis, P., Vrekoussis, M., Putaud, J.P., Mihalopoulos, N., 2006. Origin and variability of particulate matter (PM10) mass concentrations over the Eastern Mediterranean. Atmos. Environ. 40, 4679–4690I. https://doi.org/10.1016/j.atmosenv.2006.04.020.

Gobcan, Datos on-line de la Red de Control y Vigilancia de la Calidad del Aire de Canarias. https://www3.gobiernodecanarias.org/medioambiente/calidaddelaire/inicio.do.

Gonzalez-Martin, C., Coronado-Alvarez, N.M., Teigell-Perez, N., Diaz-Solano, R., Exposito, F.J., Diaz, J.P., Griffin, D.W., Valladares, B., 2018. Analysis of the impact of African dust storms on the presence of enteric Viruses in the atmosphere in Tenerife, Spain. Aerosol Air Qual. Res. 18, 1863–1873I. https://doi.org/10.4209/aaqr.2017.11.0463.

González-Martín, C., Pérez-González, C.J., González-Toril, E., Expósito, F.J., Aguilera, Á., Díaz, J.P., 2021. Airborne Bacterial community composition according to their origin in Tenerife, canary islands. Front. Microbiol. 12 https://doi.org/10.3389/fmicb.2021.732961.

Gordo, E., Dueñas, C., Fernández, M.C., Liger, E., Cañete, S., 2015a. Behavior of ambient concentrations of natural radionuclides 7Be, 210Pb, 40K in the Mediterranean coastal city of Málaga (Spain). Environ. Sci. Pollut. Control Ser. 22, 7653–7664I. https://doi.org/10.1007/s11356-014-4039-5.

Gordo, E., Liger, E., Dueñas, C., Fernández, M.C., Cañete, S., Pérez, M., 2015b. Study of 7Be and 210Pb as radiotracers of African intrusions in Malaga (Spain). J. Environ. Radioact. 148, 141–153I. https://doi.org/10.1016/j.jenvrad.2015.06.028.

Goudie, A.S., Middleton, N.J., 2001. Saharan dust storms: nature and consequences. Earth Sci. Rev. 56, 179–204I. https://doi.org/10.1016/S0012-8252(01)00067-8.

Hamadneh, H.S., Ababneh, Z.Q., Hamasha, K.M., Ababneh, A.M., 2015. The radioactivity of seasonal dust storms in the Middle East: the May 2012 case study in Jordan. J. Environ. Radioact. 140, 65–69I. https://doi.org/10.1016/j.jenvrad.2014.11.003.

Hernández, F., Alonso-Pérez, S., Hernández-Armas, J., Cuevas, E., Karlsson, L., Romero-Campos, P.M., 2005a. Influence of major African dust intrusions on the 137Cs and 40K activities in the lower atmosphere at the Island of Tenerife. Atmos. Environ. 39, 4111–4118I. https://doi.org/10.1016/j.atmosenv.2005.03.032.

Hernández, F., Hernández-Armas, J., Catalán, A., Fernández-Aldecoa, J.C., Karlsson, L., 2005b. Gross alpha, gross beta activities and gamma emitting radionuclides composition of airborne particulate samples in an oceanic island. Atmos. Environ. 39, 4057–4066I. https://doi.org/10.1016/j.atmosenv.2005.03.035.

Hernandez, F., Karlsson, L., Hernandez-Armas, J., 2007. Impact of the tropical storm Delta on the gross alpha, gross beta, 90Sr, 210Pb, 7Be, 40K and 137Cs activities measured in atmospheric aerosol and water samples collected in Tenerife (Canary Islands). Atmos. Environ. 41, 4940–4948I. https://doi.org/10.1016/j.atmosenv.2007.01.054.

Hernandez, F., Rodríguez, S., Karlsson, L., Alonso-Pérez, S., López-Pérez, M., Hernandez-Armas, J., Cuevas, E., 2008. Origin of observed high 7Be and mineral dust concentrations in ambient air on the Island of Tenerife. Atmos. Environ. 42, 4247–4256I. https://doi.org/10.1016/j.atmosenv.2008.01.017.

Huang, Y.-J., Tao, Y.-L., Lin, J., Shang-Guan, Z.-H., 2009. Annual cycle of gross β activities in aerosol around Daya Bay area, China. Chemosphere 75, 929–933I. https://doi.org/10.1016/j.chemosphere.2009.01.022.

Igarashi, Y., Aoyama, M., Hirose, K., Povinec, P., Yabuki, S., 2005. What anthropogenic radionuclides (90Sr and 137Cs in atmospheric deposition, surface soils and aeolian dusts suggest for dust transport over Japan. Water, Air, & Soil Pollution: Focus 5, 51–69I. https://doi.org/10.1007/s11267-005-0726-z.

IPCC, 2014. In: Pachauri, R.K., Meyer, L.A. (Eds.), Climate Change 2014: Synthesis Report. Contribution of Working Groups I, II and III to the Fifth Assessment Report of the Intergovernmental Panel on Climate Change [Core Writing Team. IPCC, Geneva, Switzerland, p. 151.

Junta_Andalucia, Calidad del aire. https://www.juntadeandalucia.es/medioambiente/portal/areas-tematicas/atmosfera/la-calidad-del-aire.

Karanasiou, A., Moreno, N., Moreno, T., Viana, M., de Leeuw, F., Querol, X., 2012. Health effects from Sahara dust episodes in Europe: Literature review and research gaps. Environ. Int. 47, 107–114I. https://doi.org/10.1016/j.envint.2012.06.012.

Karlsson, L., Hernandez, F., Rodríguez, S., López-Pérez, M., Hernandez-Armas, J., Alonso-Pérez, S., Cuevas, E., 2008. Using 137Cs and 40K to identify natural Saharan dust contributions to PM10 concentrations and air quality impairment in the Canary Islands. Atmos. Environ. 42, 7034–7042I. https://doi.org/10.1016/j.atmosenv.2008.06.016.

Kaufman, Y.J., Tanré, D., Boucher, O., 2002. A satellite view of aerosols in the climate system. Nature 419, 215–223I. https://doi.org/10.1038/nature01091.

Koçak, M., Mihalopoulos, N., Kubilay, N., 2007. Contributions of natural sources to high PM10 and PM2.5 events in the eastern Mediterranean. Atmos. Environ. 41, 3806–3818I. https://doi.org/10.1016/j.atmosenv.2007.01.009.

Kulan, A., 2006. Seasonal 7Be and 137Cs activities in surface air before and after the Chernobyl event. J. Environ. Radioact. 90, 140–150I. https://doi.org/10.1016/j.jenvrad.2006.06.010.

Liu, Q., Huang, Z., Hu, Z., Dong, Q., Li, S., 2022. Long-range transport and evolution of Saharan dust over east Asia from 2007 to 2020. J. Geophys. Res. Atmos. 127, e2022JD036974I https://doi.org/10.1029/2022JD036974.

López-García, P., Gelado-Caballero, M.D., Santana-Castellano, D., Suárez de Tangil, M., Collado-Sánchez, C., Hernández-Brito, J.J., 2013. A three-year time-series of dust deposition flux measurements in Gran Canaria, Spain: a comparison of wet and dry surface deposition samplers. Atmos. Environ. 79, 689–694I. https://doi.org/10.1016/j.atmosenv.2013.07.044.

López-Pérez, M., Ramos-López, R., Perestelo, N.R., Duarte-Rodriguez, X., Bustos, J.J., Alonso-Pérez, S., Cuevas, E., Hernández-Armas, J., 2013. Arrival of radionuclides released by the Fukushima accident to Tenerife (canary islands). J. Environ. Radioact. 116, 180–186I. https://doi.org/10.1016/j.jenvrad.2012.09.011.

López-Pérez, M., Lorenzo-Salazar, J.M., Expósito, F.J., Díaz, J.P., Salazar, P., 2020. Impact of a massive dust storm on the gross alpha, gross beta, 40K, 137Cs, 210Pb, 7Be activities measured in atmospheric aerosols collected in Tenerife, Canary Islands. Atmos. Environ. 239, 117806I. https://doi.org/10.1016/j.atmosenv.2020.117806.

López-Pérez, M., Martín-Luis, C., Hernández, F., Liger, E., Fernández-Aldecoa, J.C., Lorenzo-Salazar, J.M., Hernández-Armas, J., Salazar-Carballo, P.A., 2021. Natural and artificial gamma-emitting radionuclides in volcanic soils of the Western Canary Islands. J. Geochem. Explor. 229, 106840I. https://doi.org/10.1016/j.gexplo.2021.106840.

López-Pérez, M., Hernández, F., Liger, E., Gordo, E., Fernández-Aldecoa, J.C., Expósito, F.J., Díaz, J.P., Hernández-Armas, J., Salazar-Carballo, P.A., 2022. Cs-134 in soils of the western canary islands after the Chernobyl nuclear accident. J. Geochem. Explor. 242, 107085I. https://doi.org/10.1016/j.gexplo.2022.107085.

Masson, O., Pourcelot, L., Gurriaran, R., Paulat, P., 2005. Radioecological impact of Saharan dusts fallout. Case study of a major event on the 21. of february 2004 in south part of France; Impact radioecologique des retombees de poussieres sahariennes. Episode majeur du 21/02/2004 dans le sud de la France, vol. 92. Institut de Radioprotection et de Surete Nucleaire (IRSN), France. Clamart (France).

Masson, O., Piga, D., Gurriaran, R., D'Amico, D., 2010. Impact of an exceptional Saharan dust outbreak in France: PM10 and artificial radionuclides concentrations in air and in dust deposit. Atmos. Environ. 44, 2478–2486I. https://doi.org/10.1016/j.atmosenv.2010.03.004.

Menut, L., Masson, O., Bessagnet, B., 2009. Contribution of Saharan dust on radionuclide aerosol activity levels in Europe? The 21–22 February 2004 case study. J. Geophys. Res. Atmos. 114 https://doi.org/10.1029/2009JD011767.

Michaelides, S., Karacostas, T., Sánchez, J.L., Retalis, A., Pytharoulis, I., Homar, V., Romero, R., Zanis, P., Giannakopoulos, C., Bühl, J., Ansmann, A., Merino, A., Melcón, P., Lagouvardos, K., Kotroni, V., Bruggeman, A., López-Moreno, J.I., Berthet, C., Katragkou, E., Tymvios, F., Hadjimitsis, D.G., Mamouri, R.-E., Nisantzi, A., 2018. Reviews and perspectives of high impact atmospheric processes in the Mediterranean. Atmos. Res. 208, 4–44I. https://doi.org/10.1016/j.atmosres.2017.11.022.

Mitsakou, C., Kallos, G., Papantoniou, N., Spyrou, C., Solomos, S., Astitha, M., Housiadas, C., 2008. Saharan dust levels in Greece and received inhalation doses. Atmos. Chem. Phys. 8, 7181–7192I. https://doi.org/10.5194/acp-8-7181-2008.

Moreno, T., Querol, X., Castillo, S., Alastuey, A., Cuevas, E., Herrmann, L., Mounkaila, M., Elvira, J., Gibbons, W., 2006. Geochemical variations in aeolian mineral particles from the Sahara–Sahel dust Corridor. Chemosphere 65, 261–270I. https://doi.org/10.1016/j.chemosphere.2006.02.052.

NASA, Modern-Era Retrospective Analysis for Research and Applications, Version 2. https://gmao.gsfc.nasa.gov/reanalysis/MERRA-2/.

Papayannis, A., Amiridis, V., Mona, L., Tsaknakis, G., Balis, D., Bösenberg, J., Chaikovski, A., De Tomasi, F., Grigorov, I., Mattis, I., Mitev, V., Müller, D., Nickovic, S., Pérez, C., Pietruczuk, A., Pisani, G., Ravetta, F., Rizi, V., Sicard, M., Trickl, T., Wiegner, M., Gerding, M., Mamouri, R.E., D'Amico, G., Pappalardo, G., 2008. Systematic lidar observations of Saharan dust over Europe in the frame of EARLINET (2000–2002). J. Geophys. Res. Atmos. 113 https://doi.org/10.1029/2007JD009028.

Pey, J., Querol, X., Alastuey, A., Forastiere, F., Stafoggia, M., 2013. African dust outbreaks over the Mediterranean Basin during 2001–2011: PM_{10} concentrations, phenomenology and trends, and its relation with synoptic and mesoscale meteorology. Atmos. Chem. Phys. 13, 1395–1410I. https://doi.org/10.5194/acp-13-1395-2013.

Pham, M.K., Rosa, J.J.L., Lee, S.H., Oregioni, B., Povinec, P.P., 2005. Deposition of Saharan dust in Monaco rain 2001–2002: radionuclides and elemental composition. Phys. Scripta 14I. https://doi.org/10.1238/Physica.Topical.118a00014, 2005.

Pham, M.K., Chamizo, E., Mas Balbuena, J.L., Miquel, J.-C., Martín, J., Osvath, I., Povinec, P.P., 2017. Impact of Saharan dust events on radionuclide levels in Monaco air and in the water column of the northwest Mediterranean Sea. J. Environ. Radioact. 166, 2–9I. https://doi.org/10.1016/j.jenvrad.2016.04.014.

Pham, M.K., Chamizo, E., Lopéz-Lora, M., Martín, J., Osvath, I., Povinec, P.P., 2020. Impact of Saharan dust events on radionuclides in the atmosphere, seawater, and sediments of the northwest Mediterranean Sea. J. Environ. Radioact. 214 (215), 106157I. https://doi.org/10.1016/j.jenvrad.2020.106157.

Polymenakou, P.N., Mandalakis, M., Stephanou, E.G., Tselepides, A., 2008. Particle size distribution of airborne microorganisms and Pathogens during an intense African

dust event in the eastern Mediterranean. Environmental Health Perspectives 116, 292–296I. https://doi.org/10.1289/ehp.10684.
Prospero, J.M., Nees, R.T., 1986. Impact of the North African drought and El Niño on mineral dust in the Barbados trade winds. Nature 320, 735–738I. https://doi.org/10.1038/320735a0.
Prospero, J.M., Ginoux, P., Torres, O., Nicholson, S.E., Gill, T.E., 2002. Environmental CHARACTERIZATION OF global sources OF atmospheric soil dust identified with the NIMBUS 7 total OZONE MAPPING SPECTROMETER (TOMS) ABSORBING aerosol PRODUCT. Rev. Geophys. 40, 2–31I. https://doi.org/10.1029/2000RG000095, 2-1.
Prospero, J.M., Delany, A.C., Delany, A.C., Carlson, T.N., 2021. The Discovery of African dust transport to the western Hemisphere and the Saharan air layer: a history. Bull. Am. Meteorol. Soc. 102, E1239–E1260I. https://doi.org/10.1175/BAMS-D-19-0309.1.
Querol, X., Alastuey, A., Pey, J., Cusack, M., Pérez, N., Mihalopoulos, N., Theodosi, C., Gerasopoulos, E., Kubilay, N., Koçak, M., 2009a. Variability in regional background aerosols within the Mediterranean. Atmos. Chem. Phys. 9, 4575–4591I. https://doi.org/10.5194/acp-9-4575-2009.
Querol, X., Pey, J., Pandolfi, M., Alastuey, A., Cusack, M., Pérez, N., Moreno, T., Viana, M., Mihalopoulos, N., Kallos, G., Kleanthous, S., 2009b. African dust contributions to mean ambient PM10 mass-levels across the Mediterranean Basin. Atmos. Environ. 43, 4266–4277I. https://doi.org/10.1016/j.atmosenv.2009.06.013.
Querol, X., Tobías, A., Pérez, N., Karanasiou, A., Amato, F., Stafoggia, M., Pérez García-Pando, C., Ginoux, P., Forastiere, F., Gumy, S., Mudu, P., Alastuey, A., 2019. Monitoring the impact of desert dust outbreaks for air quality for health studies. Environ. Int. 130, 104867I. https://doi.org/10.1016/j.envint.2019.05.061.
Rodríguez, S., Querol, X., Alastuey, A., Kallos, G., Kakaliagou, O., 2001. Saharan dust contributions to PM10 and TSP levels in Southern and Eastern Spain. Atmos. Environ. 35, 2433–2447I. https://doi.org/10.1016/S1352-2310(00)00496-9.
Rodríguez, S., Querol, X., Alastuey, A., Viana, M.a.-M., Alarcón, M., Mantilla, E., Ruiz, C. R., 2004. Comparative PM10–PM2.5 source contribution study at rural, urban and industrial sites during PM episodes in Eastern Spain. Sci. Total Environ. 328, 95–113I. https://doi.org/10.1016/S0048-9697(03)00411-X.
Rodríguez, S., Alastuey, A., Alonso-Pérez, S., Querol, X., Cuevas, E., Abreu-Afonso, J., Viana, M., Pérez, N., Pandolfi, M., de la Rosa, J., 2011. Transport of desert dust mixed with North African industrial pollutants in the subtropical Saharan Air Layer. Atmos. Chem. Phys. 11, 6663–6685I. https://doi.org/10.5194/acp-11-6663-2011.
Rodríguez, S., Calzolai, G., Chiari, M., Nava, S., García, M.I., López-Solano, J., Marrero, C., López-Darias, J., Cuevas, E., Alonso-Pérez, S., Prats, N., Amato, F., Lucarelli, F., Querol, X., 2020. Rapid changes of dust geochemistry in the Saharan Air Layer linked to sources and meteorology. Atmos. Environ. 223, 117186I. https://doi.org/10.1016/j.atmosenv.2019.117186.
Rodriguez-Navarro, C., di Lorenzo, F., Elert, K., 2018. Mineralogy and physicochemical features of Saharan dust wet deposited in the Iberian Peninsula during an extreme red rain event. Atmos. Chem. Phys. 18, 10089–10122I. https://doi.org/10.5194/acp-18-10089-2018.
Sala, J.Q., Cantos, J.O., Chiva, E.M., 1996. Red dust rain within the Spanish Mediterranean area. Climatic Change 32, 215–228I. https://doi.org/10.1007/BF00143711.
Salvador, P., Alonso-Pérez, S., Pey, J., Artíñano, B., de Bustos, J.J., Alastuey, A., Querol, X., 2014. African dust outbreaks over the western Mediterranean Basin: 11-year characterization of atmospheric circulation patterns and dust source areas. Atmos. Chem. Phys. 14, 6759–6775I. https://doi.org/10.5194/acp-14-6759-2014.
Scheuvens, D., Schütz, L., Kandler, K., Ebert, M., Weinbruch, S., 2013. Bulk composition of northern African dust and its source sediments — a compilation. Earth Sci. Rev. 116, 170–194I. https://doi.org/10.1016/j.earscirev.2012.08.005.
Sicard, M., Barragan, R., Dulac, F., Alados-Arboledas, L., Mallet, M., 2016. Aerosol optical, microphysical and radiative properties at regional background insular sites in the western Mediterranean. Atmos. Chem. Phys. 16, 12177–12203I. https://doi.org/10.5194/acp-16-12177-2016.
Stein, A.F., Draxler, R.R., Rolph, G.D., Stunder, B.J.B., Cohen, M.D., Ngan, F., 2015. NOAA's HYSPLIT atmospheric transport and dispersion modeling system. Bull. Am. Meteorol. Soc. 96, 2059–2077I. https://doi.org/10.1175/BAMS-D-14-00110.1.
Terray, L., D'Amico, D., Masson, O., Sabroux, J.-C., 2020. What can gross alpha/beta activities tell about 210Po and 210Pb in the atmosphere? J. Environ. Radioact. 225, 106437I. https://doi.org/10.1016/j.jenvrad.2020.106437.
Titos, G., Ealo, M., Pandolfi, M., Pérez, N., Sola, Y., Sicard, M., Comerón, A., Querol, X., Alastuey, A., 2017. Spatiotemporal evolution of a severe winter dust event in the western Mediterranean: aerosol optical and physical properties. J. Geophys. Res. Atmos. 122, 4052–4069I. https://doi.org/10.1002/2016JD026252.
Tobías, A., Pérez, L., Díaz, J., Linares, C., Pey, J., Alastruey, A., Querol, X., 2011. Short-term effects of particulate matter on total mortality during Saharan dust outbreaks: a case-crossover analysis in Madrid (Spain). Sci. Total Environ. 412–413, 386–389I. https://doi.org/10.1016/j.scitotenv.2011.10.027.
UNSCEAR, 2000. Report to the General Assembly, with Scientific Annexes. United Nations, New York, pp. 84–156.
Valenzuela, A., Olmo, F.J., Lyamani, H., Antón, M., Quirantes, A., Alados-Arboledas, L., 2012. Aerosol radiative forcing during African desert dust events (2005–2010) over Southeastern Spain. Atmos. Chem. Phys. 12, 10331–10351I. https://doi.org/10.5194/acp-12-10331-2012.
Varga, G., 2020. Changing nature of Saharan dust deposition in the Carpathian basin (central Europe): 40 years of identified north African dust events (1979–2018). Environ. Int. 139, 105712I. https://doi.org/10.1016/j.envint.2020.105712.
Varga, G., Kovács, J., Újvári, G., 2013. Analysis of Saharan dust intrusions into the Carpathian basin (central Europe) over the period of 1979–2011. Global Planet. Change 100, 333–342I. https://doi.org/10.1016/j.gloplacha.2012.11.007.
Viana, M., Querol, X., Alastuey, A., Cuevas, E., Rodríguez, S., 2002. Influence of African dust on the levels of atmospheric particulates in the Canary Islands air quality network. Atmos. Environ. 36, 5861–5875I. https://doi.org/10.1016/S1352-2310(02)00463-6.
White, J.R., Cerveny, R.S., Balling, R.C., 2012. Seasonality in European red Dust/"Blood" rain events. Bull. Am. Meteorol. Soc. 93, 471–476I. https://doi.org/10.1175/BAMS-D-11-00142.1.
WMO, Regional Center for Northern Africa, Middle East and Europe, Conducting Research and Providing Operational Products. https://dust.aemet.es/.
Who. New WHO global air quality Guidelines aim to Save Millions of Lives from air pollution. Air pollution is one of the biggest environmental threats to human health alongside climate change. https://www.who.int/news/item/22-09-2021-new-who-global-air-quality-guidelines-aim-to-save-millions-of-lives-from-air-pollution.
Zalewska, T., Biernacik, D., 2022. Be-7 and Pb-210 in fallout and aerosols in 2000–2016 in central Europe — deposition velocity and dependence on meteorological parameters. Sci. Total Environ. 826, 154205I. https://doi.org/10.1016/j.scitotenv.2022.154205.